EVALUATE H2RI WICKING FABRIC FOR PAVEMENT APPLICATION – YEAR 2
FINAL PROJECT REPORT

by
Xiong Zhang, Ph.D., P.E., Associate Professor
Department of Civil and Environmental Engineering
University of Alaska Fairbanks

Billy Connor, P.E.
Department of Civil and Environmental
Engineering University of Alaska Fairbanks

Sponsorship
Pacific Northwest Transportation Consortium
for
Pacific Northwest Transportation Consortium (PacTrans)
USDOT University Transportation Center for Federal Region 10
University of Washington
More Hall 112, Box 352700
Seattle, WA 98195-2700
In cooperation with US Department of Transportation-Research and Innovative Technology Administration (RITA)

Disclaimer

The contents of this report reflect the views of the authors, who are responsible for the facts and the accuracy of the information presented herein. This document is disseminated under the sponsorship of the U.S. Department of Transportation's University Transportation Centers Program, in the interest of information exchange. The Pacific Northwest Transportation Consortium, the U.S. Government and matching sponsor assume no liability for the contents or use thereof.

Technical Report Documentation Page

1. Report No.	2. Government Accession No.	3. Recipient's Catalog No.
2013-S-UAF-0026	01497959	

4. Title and Subtitle	5. Report Date
Evaluate H2RI Wicking Fabric for Pavement Applications	10/31/2015
	6. Performing Organization Code INE/PacTrans 15.12
Xiong Zhang, and Billy Connor	**8. Performing Organization Report No.** INE/PacTrans 15.12
9. Performing Organization Name and Address PacTrans Pacific Northwest Transportation Consortium University Transportation Center for Region 10 University of Washington More Hall 112 Seattle, WA 98195-2700 Alaska University Transportation Center P.O. Box 755900 Fairbanks, AK 99775-5900	**10. Work Unit No. (TRAIS)** **11. Contract or Grant No.** G00008085
12. Sponsoring Organization Name and Address United States of America Department of Transportation Research and Innovative Technology Administration Alaska Department of Transportation & Public Facilities Research, Development, and Technology Transfer 2301 Peger Road Fairbanks, AK 99709-5399	**13. Type of Report and Period Covered** Research: July 1, 2013 to October 31, 2015 **14. Sponsoring Agency Code**
15. Supplementary Notes Report uploaded at www.pacTrans.org	

16. Abstract

The Tencate H2Ri wicking fabric has proven to work well on two roadway sections on the Dalton Highway. In each the fabric has reduce the water content in the embankment resulting in a maintenance free section. This project used a 24 foot flume in the laboratory to evaluate the effectiveness of the fabric on well graded sand and organic silt. The fabric effectively removed the moisture in the well graded sand. However, the organic silt blinded the wicking fibers which eliminated the capillary moisture movement. The results also demonstrated that overlapping the fabric for joints is not efficient.

17. Key Words	18. Distribution Statement
Geotextiles (Rbmdxcet), Geosynthetics (Rbmdxce), Woven fabrics (Rbmdxcxf)	No restrictions.

19. Security Classification (of this report)	20. Security Classification (of this page)	21. No. of Pages	22. Price
Unclassified.	Unclassified.	56	NA

Form DOT F 1700.7 (8-72) **Reproduction of completed page authorized**

Table of Contents

List of Figures

List of Tables

CHAPTER 1 INTRODUCTION

H2Ri wicking fabric is gaining popularity for removing moisture from roadway embankments. Alaska's first experience was at Beaver Slide, Mile 110.5 on the Dalton Highway. Beaver slide had been problematic since its construction in 1975. The site is situated on a side hill cut with a roadway grade exceeding 6%. The soil at Beaver Slide is a sand with about 6 % passing the #200 sieve. This combination caused water to move across and along the roadway causing wet soft spots in the roadway. Freeze-thaw caused exacerbated the problem. The installation of H2Ri eliminated the problem. After 5 years, the roadway has been free of soft spots.

The Alaska Department of Transportation and Public Facilities (DOT&PF) use H2Ri on another Dalton Highway project at MP 119. To date that roadway has also worked well. However, DOT&PF has asked two questions:

1. What are the limitations of soil types that H2Ri can be expected to work?
2. Will the product continue to work when the length requirements exceed the width of the wicking fabric?

This study is designed to answer those two questions. Two materials were used to represent the extremes for which H2Ri might be used. The first is clean uniform sand that is free draining. This will provide an understanding of how well the material works in a permeable soil.

The second material was organic silt obtained from the Permafrost Tunnel near Fox Alaska, just north of Fairbanks. This soil is essentially impermeable providing an understanding of the performance of the material under these conditions.

CHAPTER 2 LITERATURE REVIEW

2.1 Adverse Effects of Subsurface Water in Pavement Design

Excessive water in a pavement structure is recognized as one of the major adverse factors that influence its overall performance. It can cause a variety of engineering problems, for instance,

causing soil expansion and collapsing, reducing the soil strength and stiffness, increasing excess pore water pressure and developing seepage forces, stripping asphalt pavement and generating cracks (Han and Zhang, 2014). Figure 2.1 shows the mechanism of water-induced Asphalt Concrete (AC) pavement distress (Taylor and Khosla, 1984). Both dynamic traffic load and thermal shrinkage induce cracks within the asphalt pavement layer. The cracks partially or completely filled with water through infiltration. This will result in base and subgrade materials saturation with time. Higher pore water pressure is induced by large dynamic loading of heavy duty vehicles. In consequence, free water within the base and subgrade together with fines will be squeezed out of the pavement structure and this phenomenon is called pumping. Free water wedges are produced beneath the asphalt pavement. Wet softened area due to loss of fines in the base and subgrade layers causes potholes or depressions of the pavement structure. Similar pumping phenomena also occurs in Portland Cement Concrete (PCC) pavements (Mallela et al., 2000), as shown in Figure 2.2. Upward curls of pavement slabs (resulting from uneven temperatures above and beneath cement pavement slab) tend to create small pores. Free water can easily penetrates and saturates base and subgrade layers via joints through precipitation and infiltration. The upcoming wheel load first causes the backward slab edge deflecting downward and generates large pore water pressure. When the wheel passes the joint, the forward slab deflects downward and previous backward slab rebounds upward. The cyclic downward deflecting- upward rebounding process pumps water out of the pavement structure together with fines. The materials beneath the joints of slabs erode with time, and fault or crack near joint will further accelerate the deteriorating process.

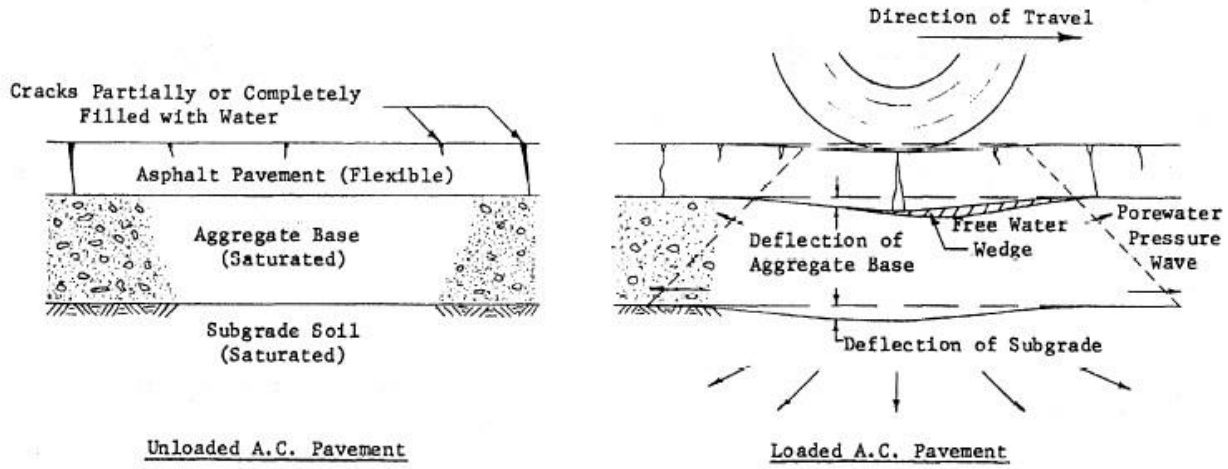

Figure 2.1 Adverse Effects of Water on Asphalt Concrete (AC) Pavement

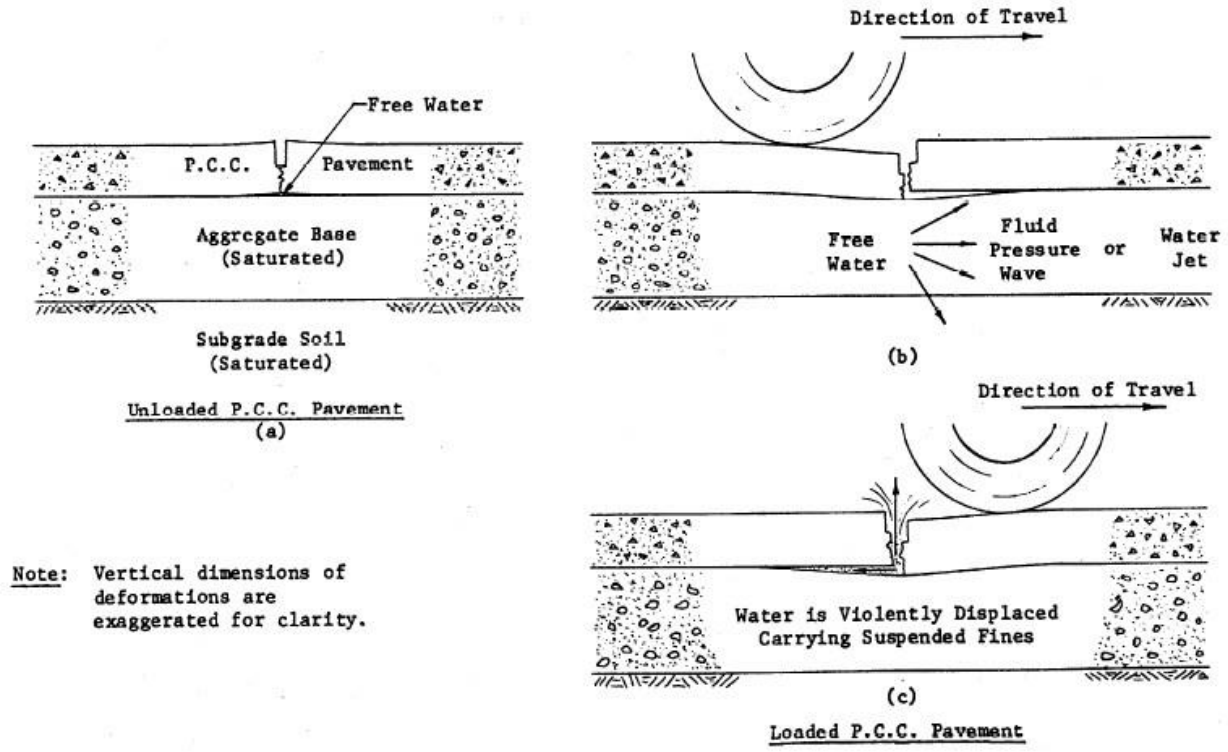

Figure 2.2 Adverse Effects of Water on Portland Cement Concrete (PCC) Pavement

Another adverse effect of water on pavement structure is called “frost boiling”, which causes extensive damage in northern regions or cold climates. The mechanism of “frost boiling” phenomena is related to frost heave and thaw weakening processes (Chamberlain, 1987), as

shown in Figure 2.3. For coarse grained base, subbase and subgrade courses, the water can be drained out fairly fast. However, when encountered courses with more fines, the fine content is susceptible to intrude up into the base layer due to dynamic traffic load and water migration will and causes differential settlement. Frost heave is attributed to the formation of ice lenses during freezing. Three key elements are required in ice lenses formation: (1) frost susceptible (FS) soils, (2) subfreezing temperature and (3) available water sources. FS soils are defined as soils with pore sizes between particles and particle surface area that promote capillary flow (Casagrande, 1947 and 1987; Csathy and Townsend, 1962). For engineering practice, soils contain over 10% fines are considered as FS soils. During freezing period, water in large void space freezes into ice crystals as freezing front moving downward. Water expands about 9% by volume and is considered as impermeable when frozen. Negative pore water pressure was generated and ice crystals tend to attract water from adjacent voids. However, the frozen soil above the freezing front is impermeable and the only available water source comes from the unfrozen subgrade that beneath the freezing plane. As crystals continue to grow and are fed by capillary movement through FS soils, shallow groundwater continuously flows upward to the freezing plane. This will cause pavement to heave and sometimes crack. As the upcoming spring comes, the ice lenses start to melt and cause softer areas within the pavement structure (Taber, 1930 a and b, 1978 and 1980). When water is drained out with time, the differential settlement phenomena can be observed. Soft and weak soils provide limited friction and interlock between subgrade and base materials and result in rutting issues.

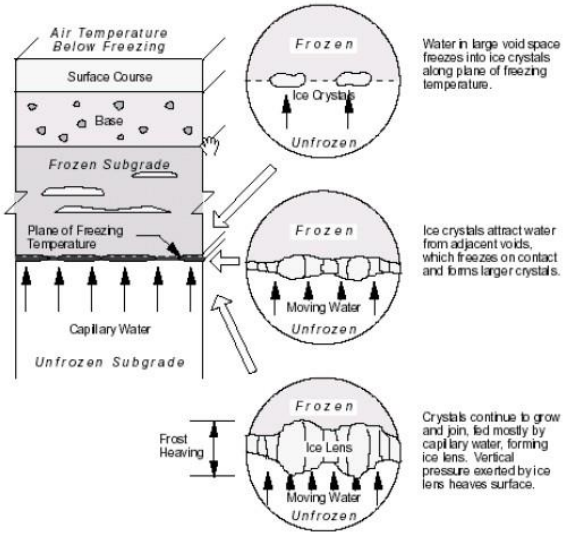

Figure 2.3 Ice Lenses Formation

2.2 Types and Sources of Subsurface Water

The subsurface water exists in 4 forms: water vapor, bounded water, capillary water and free (or gravitational water) (Kochina and Ya, 1952; Aravin and Numerov, 1953 and Muskat, 1946). The water vapor in most cases stores inside soil pores where above the saturation zone. In the existing subdrainage design methods, water vapor transmission is negligible. For bounded water, it is relatively hard to move from the soil particles and can be considered as part of the soil particles. This part of the water phase in soil also cannot move under gravity force and therefore is not considered in most subdrainage design methods. Capillary water also exists in the soil pores where above the saturation zone. However, different from water vapor, it can flow under the action of surface tension. The height of capillary rise is a function of the soil particle distribution, which relates to soil particle size distribution and density (Lane and Washburn, 1946; Barber and Sawyer, 1952). Since capillary water cannot be drained out by gravity, the most common way to control capillary water is to lower the water table or use capillary barrier, which blocks the upward capillary flow. Last but the most common type of water, namely free water, is the water in liquid form that flows under the force of gravity and obeys Darcy's law. Control free water becomes the major concern in the existing subdrainage design methods.
The subsurface water comes from a variety of sources and mainly falls into two categories: groundwater and infiltration (Brown et al., 2001). Groundwater refers to the water exists in the saturation zone below the water table. The major source of groundwater is precipitation. Infiltration water is defined as the water seeps into the pavement structure through pavement surface, shoulders or median. Precipitation is also the major source for infiltration water. For bituminous pavements, the primary infiltration water source is longitudinal joints at shoulders and construction joints between strips of paving. As for concrete slabs, infiltration water takes place through cracks, joints and shoulders (Cedergren, 1974 and Cedergren et al., 1973).

2.3 Conventional Drainage Design Methods

In order to obtain sufficient pavement drainage, the major design considerations involve: preventing the amount of water entering the pavement structure and quickly removing water that enters the pavement system, using materials that are insensitive to the effect of moisture, and incorporating design methods to minimize water damage (MEPDG, 2004; FHWA, 1980 and AASHTO 1993). One design method to minimize surface infiltration is to provide adequate longitudinal and cross slopes. The less time the water detained on the road surface, the less amount of water can infiltrate into pavements through joints and cracks. Another common method is to seal joins, cracks and all other discontinuities that allow water to infiltrate into the pavement structure. Except for those two methods, moisture insensitive materials, such as ATB (Asphalt Treated Base), CTB (Cement Treated Base) and granular materials with less fines, are also popular in controlling the water content in pavement structures.

A subsurface drainage system can be categorized into the following 4 types: (1) longitudinal drains, (2) transverse and horizontal drains, (3) drainage blankets and (4) well systems. A longitudinal drain involves either a trench of substantial depth or a collector pipe (or protective filter) that parallel to the roadway centerline. Transverse drains run laterally beneath the roadway that are designed to drain both groundwater and infiltration water in base and subbase courses. Drainage blanket refers to a very permeable layer that can be used beneath or as an integral part of the pavement structure to remove infiltration or groundwater from both gravity and artesian sources. Although base and subbase courses are relatively permeable, they are not considered as drainage blanket layer unless they are specially designed with high coefficient of permeability, a positive outlet for water collection and with protective filter layer. System of vertical wells often been used to lower groundwater level and relieve pore water pressure. Sand filled vertical wells are commonly used to accelerate drainage of soft and compressible foundation materials (Rutledge and Johnson, 1958; Rechart, 1957).

In recognition of impact moisture can have on pavement performance, the AASHTO Design Guide incorporated an empirical drainage coefficient into design equations. Four approaches commonly employed to control or reduce moisture problems are listed below:

1. Prevent moisture from entering the pavement system. Provide adequate cross slopes and longitudinal slopes. In general, the less time the water is allowed to stay on the pavement slopes is based on the pavement surface, the less moisture can infiltrate through joints and cracks. (Anderson et al., 1998). Joint and crack sealing are required throughout the pavement service life.
2. Use materials that are insensitive to the effects of moisture, such as lean concrete base, cement treated base, asphalt treated base and gravel base with limited fines. Open-graded material allows easier movement of moisture through material.
3. Removal of free water through subsurface drainage. Consider providing three types of drainage systems: surface drainage, groundwater drainage and subsurface drainage (subdrainage). These three are only effective for free water. Water held by capillary forces in soils and in fine aggregates cannot be drained. The effects for this bound moisture are considered in the EICM through adjustments to pavement materials properties.

Mechanistic-Empirical Design Guide (FHWA, 2004) is the most commonly used pavement design guidebook. Within the Appendix SS, a comprehensive description of the drainage design method is introduced. Basically, it compares the inflow and drainage capacity to determine if the drainage design is sufficient drainage both groundwater and infiltration water quickly enough.

Estimation of Inflow

Water inflow sources include surface infiltration, ground water infiltration and meltwater (from ice lenses). Surface infiltration is the most important and should be always considered in subdrainage design. Groundwater shall be lowered by deep longitudinal drains and shall not be allowed to seep into the pavement structure. If it is not feasible, the amount of seepage entering the drainage layer shall be estimated. The meltwater from ice-lenses only need to be considered in northern climates with frost heave. Because fine grained soils are very impermeable, it is unlikely that flow from both groundwater and meltwater will occur at the same time. Therefore, only the larger of the inflows needs be considered.

The amount of infiltration is related directly to cracking. For evaluating the amount of water via infiltration, the duration of rainfall is a more critical factor than the intensity. Equation 1 is adopted to determine the infiltration rate and Figure 1 shows the isotropic precipitation rate contour.

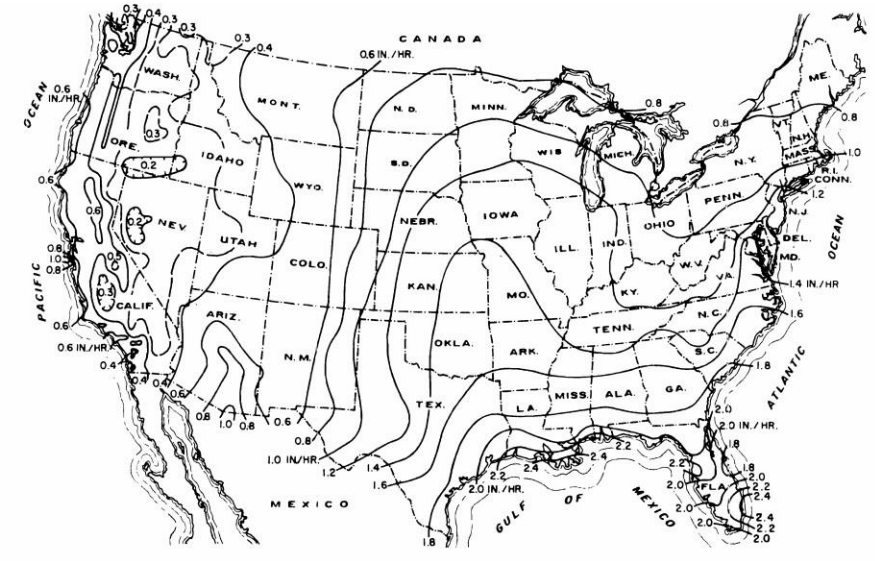

Figure 2.4 1Hour/ 1 Year Precipitation Rate

$$q_i = \left(\frac{}{W_p} + \frac{W_c}{W_p C_s}\right) + k \quad (1)$$

Where,

q_i = infiltration rate per unit area, $ft^3/hr/ft^2$;

I_c = cracking infiltration rate, 2.4 $ft^3/day/ft$;

N_c = number of longitudinal cracks;

W_p = width of pavement subjected to infiltration;

W_c = length of transverse cracks or joints;

C_s = spacing of transverse cracks or joints;

k_p = rate of infiltration through uncracked pavement surface, which is usually equal to the coefficient of permeability of HMA or PCC.

By assuming that $N_c = N + 1$, (N is number of traffic lanes), $W_c = W_p$, $k_p = 0$, infiltration rate is 0.1 $ft^3/day/ft$ of crack, the inflow rate can be written as:

$$q = q_i W = 0.1\left(N + 1 + \frac{W_p}{C_s}\right) \quad (2)$$

As for groundwater seepage, assuming the pavement bottom is an impermeable layer, the inflow is divided into two parts: inflow above the bottom of the drainage layer, q_1, and inflow below the drainage layer, q_2. The drainage layer is used to lower the water table, in addition to providing drainage for surface infiltration.

$$q_1 = \frac{(H - H_0)^2}{2L_i} \quad (3)$$

Where,

q_1 = volume of flow per unit time per unit length of the longitudinal drain, $ft^3/day/ft$;

k = permeability of the subgrade soil;

H = initial height of the groundwater table above the impervious layer;

H_0 = vertical distance between the bottom of drainage layer and the impervious layer;

L_i = distance of influence, $L_i = 3.8\ (H-H_0)$;

After q_1 has been determined, use the chart in Figure 5 to determine q_2, the lateral or horizontal flow is:

$$q_L = q_1 + q_2 \quad (4)$$

The groundwater inflow to the drainage layer per unit area is:

$$q_w = \frac{2q_2}{W} \quad (5)$$

Where,

W = width of the roadway.

However, if the pavement is sloped to one side and the collector pipes are installed only on one side, the lateral flow per unit length of pipe is:

$$q_L = 2(q_1 + q_2) \quad (6)$$

$$q_w = \frac{q_1 + 2q_2}{W} \quad (7)$$

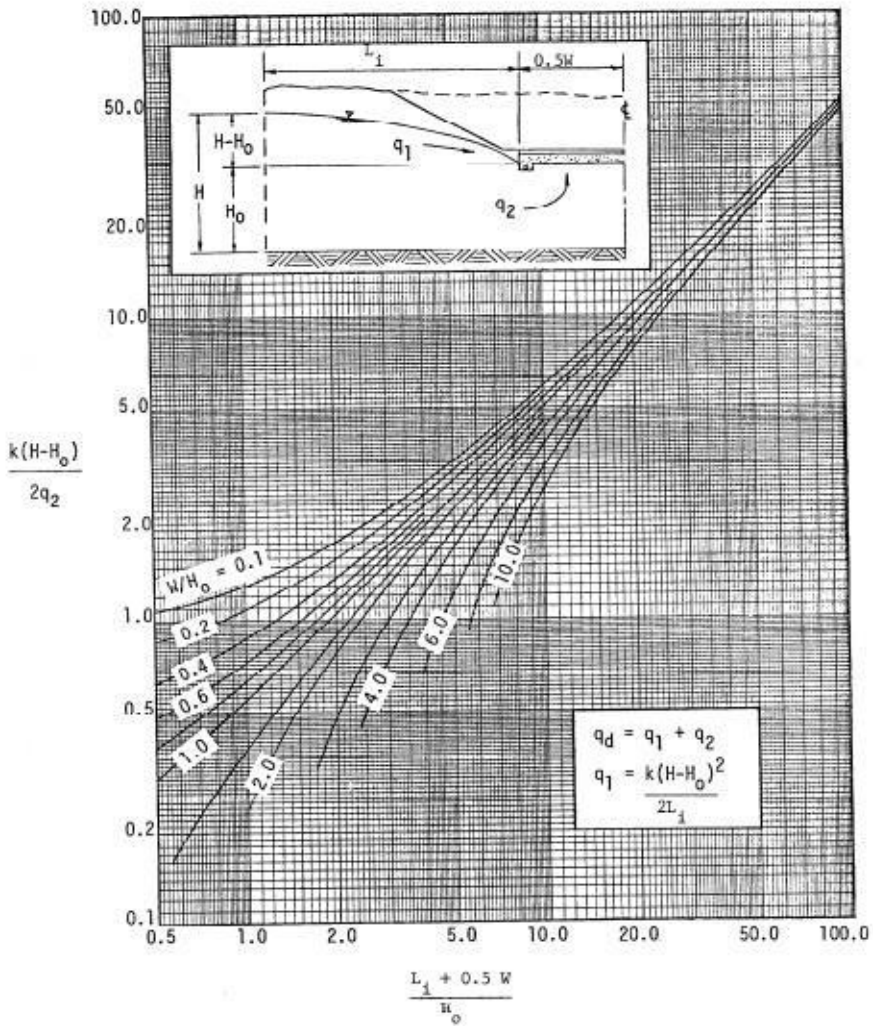

Figure 2.5 Flow Rate in Horizontal Drainage Blanket

The design inflow is the sum of inflows from all sources minus the outflow through the subgrade soil. When the subgrade is not affected by any water table, a simple and conservative method is to assume the hydraulic gradient to be 1, so the outflow rate is equal to the permeability of the soil. The outflow through subgrade depends on the permeability of the soil and on the water table at the boundary and can be determined by the use of flownet or other simplified design chart. If the outflow through the subgrade is neglected, the design inflow can be determined by one of the following combinations:

1. If there is no frost action, the design inflow, q_d, is the sum of surface infiltration q_i and groundwater flow q_g:

$q_{\blacklozenge} = q_i + q_{\blacklozenge}$ (8)

2. If there is frost action, q_d is the sum of surface infiltration qi and inflow from meltwater q_m:

$$q_{\blacksquare} = q_i + q_{\blacksquare} \quad (9)$$

Estimate Drainage Capacity

There are two design requirements for a drainage layer: (1) the steady-state capacity must be greater than the inflow rate, and (2) the unsteady-state capacity must be such that the water can be drained quickly after each precipitation event. The discharge is composed of two parts: discharge through area, H, caused by the hydraulic gradient, S; or through area H/2 caused by the hydraulic gradient H/L. When S = 0, $q = 0.5kH^2/L$, which is a direct application of Darcy's law, assuming the surface is at the top of drainage layer on one end at the bottom of the layer on the other end, which is an average flow area of H/2.

For steady-state flow:

$$q = k(\blacksquare\blacksquare + \frac{H}{2L}) \quad (10)$$

Where,

q = discharge capacity of the drainage layer;

k = permeability of the drainage layer;

S = slope of the drainage layer;

H = thickness of the drainage layer;

L = length of the drainage layer.

For unsteady-state flow:

Unsteady-state flow capacity is defined by the degree of drainage, which is a ratio between the volume of water drained since the rain stops and the total storage capacity of the drainage layer. The time for a 50% degree of drainage can be computed as:

$$t_{50} = \frac{\blacksquare L^2}{2k(H+SL)} \quad (11)$$

Where,

t_{50} = time for 50% drainage;

n_e = effective porosity, which is the porosity occupied by drainage water.

For excellent drainage, AASHTO (AASHTO, 1993) requires that the water be removed within 2 hours. For the design of drainage layer, the requirement that the time for complete or 95% drainage be less than 1h, appears to be more appropriate. The degree of drainage, U, depends on a time facto,r T_f, and a slope factor, S_f, respectively defined as:

$$\text{[illegible]} = \frac{kHt}{\text{[illegible]}L^2} \quad (12)$$

$$\text{[illegible]} = \frac{LS}{H} \quad (13)$$

2.4 Comparisons of Conventional and New Drainage Design Concept

By investigating the existing pavement drainage design methods and criteria (MEPDG, AI, Shell, and ASSHTO), they only deal with "free water" or gravitational water flow, and water detained by capillary force or in fine soils (in unsaturated conditions) cannot be drained. When a pavement structure is built, it is often built with soils at their optimum moisture contents to achieve the best performance. After construction, the surface soils are exposed to the surrounding atmospheric environment and dried quickly since the relative humidity in the air is often less than 90%. Such a relative humidity corresponds to a suction value of 140 MPa (Fredlund et al, 1993). All soils become air-dried under such high suction. Air enters the voids in the soils and the surface soils form a dried crust which has very low permeability (nearly impermeable) to transport water from inside to outside. In the meantime, the soils inside the pavement structure tend to reach equilibrium with surroundings (normally the ground water table) through capillary rise as shown in Figure 2.6.

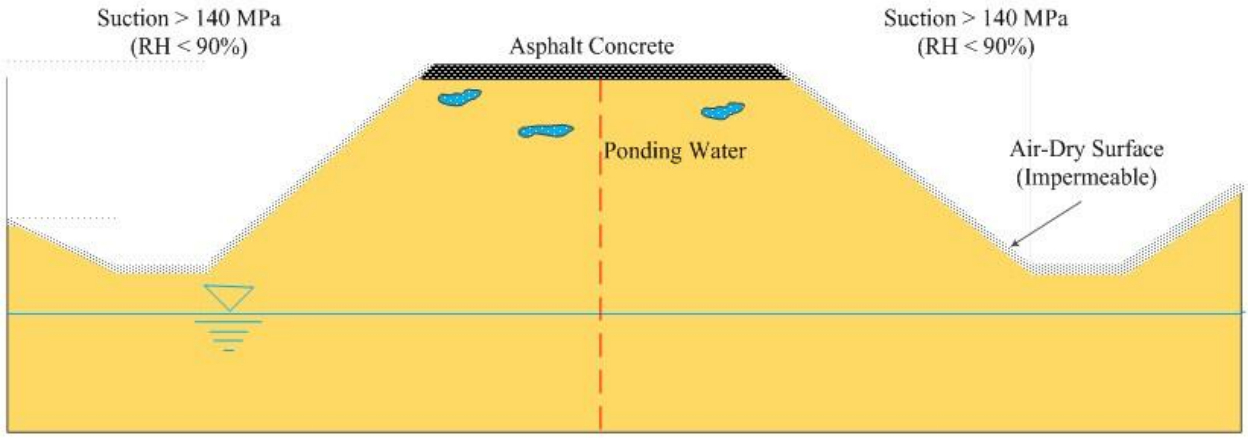

Figure 2.6 Conventional Drainage Design Concept

When surface soils are air-dry and have cracks, they have high permeability for water infiltration. The infiltrated water can be ponded in the upper part of the pavement under unsaturated conditions and leads to very low suction. Other factors such the water vapor condensation below the pavement surface during the temperature decrease in the night can also lead to water content increase in the base and sub-base materials. The pore water pressure in the soils is negative when the soils are unsaturated. Hence, the water cannot be drained by a

conventional drainage system which is typically made of granular material with large voids that relies on gravity as a driving force for drainage. Instead, air can easily enter to the large voids and block the outward liquid water flow. Although sometimes the granular materials are used as a capillary barrier for liquid water flow to mitigate the frost heave and thaw-weakening problem, they cannot prevent the water flow in the vapor form inside the embankment. Over the time, the moisture content for soils in the pavement embankment will increase even if there is a granular drainage layer. Another common way is to use geosynthetics as capillary barriers to prevent capillary flow. Geotextiles can act as capillary barriers because the suction in fine grained soils prevents water flow to larger geotextile pores. However suction decreases with increment in water content. When the suction decreases to the air entry value it ceases the geotextile as a capillary barrier. Meanwhile, the water accumulated in the overlying soils beyond levels weakens the granular base or subbase layers due to the additional moisture having stored. This could cause a problem with geotextile, geonet and geocomposite in unsaturated conditions.

In contrast, Figure 2.7 shows the new conceptual design. A layer of the wicking fabric is proposed to be installed in the base layer parallel to the pavement surface. At the two shoulders of the embankment, the wicking fabric is exposed to the atmosphere with a length of 2-3meters. Due to its hydrophilic and hygroscopic nature, the wicking fibers can absorb water from the surrounding soils inside the embankment. As discussed previously, there is big difference in the relative humidity or suctions between the soils inside the embankment and the atmosphere. This difference in relative humidity provides the driving force for the wicking fabric to suck the water out of the pavement structure to the embankment shoulder, and finally the water will be vaporized into the air to reach an equilibrium condition. Different from the conventional granular or geotextile drainage system, the wicking fibers have many micro-channels inside which can maintain being saturated under low relative humidity (or high suction value). Consequently, the wicking fabric builds up a liquid connection between the inside and outside of the pavement structure for continuous water removal. Compared with the amount of water needed to saturate the Earth's atmosphere, the amount of water in the embankment is very small. Therefore, the wicking process will continue until air enters into the micro-channels of the wicking fibers.

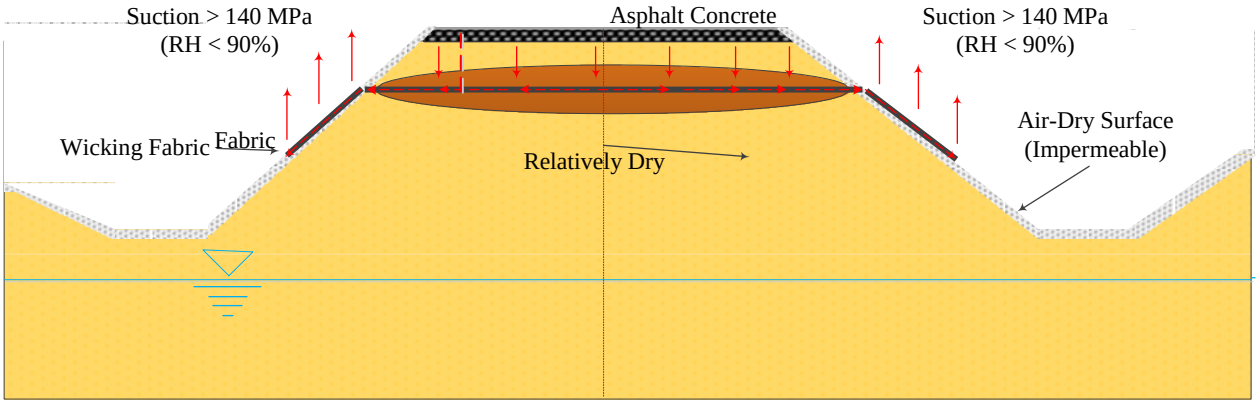

Figure 2.7 New Drainage Design Concept

2.5 Geosynthetic Application in New Drainage Design

Geosynthetics are synthetic and polymeric materials used in civil engineering. There are 8 major product categories including: geotextile, geogrid, geocell, geomembrane, geofiber, geofoam, geosynthetic clay liner and geocomposite, as shown in Figure 2.8. Geosynthetics have wide range of applications in geotechnical engineering, such as road, airfield, embankment, retaining structure and reservoir.

Geotextile and geogrid are two types of geosynthetics that most commonly used in geotechnical engineering field. The major geosynthetic functions for roadway stabilization and reinforcement are separation, confinement, soil reinforcement, filtration and drainage. Geotextile and geogrid can be used as a separation material, which is placed between two dissimilar materials and maintain the integrity of both materials. For confinement function, geotextile and geogrid can be used to prevent aggregate lateral movement, which will compromise the roadway and pavement structure performance. Geotextile takes advantage of the friction while geogrid uses interlock to mitigate the relative movement. For reinforcement function, both geotextile and geogrid works effectively to spread the load and prevent excess load on different components that make up the road.

Even though geotextile and geogrid provide separation, confinement and reinforcement functions, when it comes to filtration and drainage function. Geotextile definitely shows more advantages compared with geogrid. Geotextile allows free water to flow across the geotextile plane while controls soil particle retention. As water and small particles drain through confined layers of aggregates and subgrade, smaller particles eventually traps between bigger ones, which results in a larger grading and providing more stable layer. It is impossible to grade aggregates by using geogrid which has much larger openings.

Figure 2.8 Geosynthetic Category

2.6 Geotextile with Wicking Ability

Recently, a newly developed geotextile with lateral drainage function can potentially be used to reduce the water content within road and pavement structure, as shown in Figure 9(a). This type of geotextile is a dual functional geotextile product, which contains a high modulus polypropylene yarn for reinforcement and stabilization. The double woven layer construction provides excellent separation and filtration functions. The uniform openings also provide consistent filtration and flow characters for fine to coarse sand layer. The double layer design can also provide good confinement between base and subbase resulting in a greater load distribution and good durability performance. Different from traditional geotextile, it also includes special hydrophilic and hygroscopic 4DG^{TM} fibers that can provide wicking action through the plane of the geotextile, as shown in Figure 2.9(b). The deeply grooved cross section (Figure 2.9 (c) and (d)) provides larger surface area, thus ensure the channel to hold and transfer larger amount of water even in unsaturated conditions. The average diameter of the wicking fabric is between 30-50 μm

and the average groove spacing is between 5-12 μm. Detailed information for the geotextile hydraulic and mechanical specification can be found in Table 2.1. When properly designed, it has the potential to dehydrate the subgrade and base course under unsaturated conditions and consequently improve the performance of pavements.

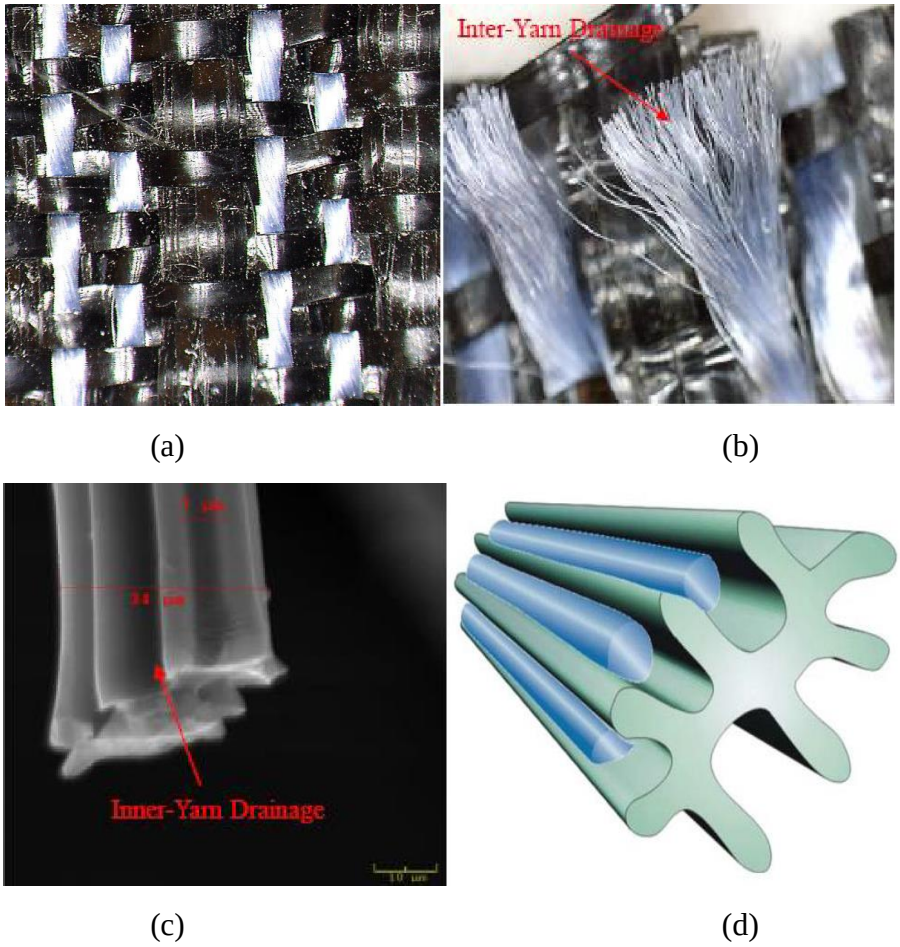

(a) (b)

(c) (d)

Figure 2.9 Innovative Geotextile with Wikcing Fabric

Table 2.1 Geotextile Specification

Mechanical Properties	Test Method	Unit	Average Roll Value
Tensile Modulus @ 2% Strain (CD)	ASTM D4595	kN/m	657
Permittivity	ASTM D4491	Sec^{-1}	0.24
Flow Rate	ASTM D4491	$l/min/m^2$	611

Pore Size (050)	ASTM D6767	Microns	85
Pore Size (095)	ASTM D6767	microns	195
Apparent Opening Size (AOS)	ASTM D4751	mm	0.43
			Tested Value
Wet Front Movement (24 minutes)	ASTM C1559	inches	6.0 Vertical Direction
Wet Front Movement (983 minutes) Zero Gradient	ASTM C1559	inches	73.3 Horizontal Direction

There are several papers regarding the lab tests about the innovative geotextile. First, TENCATE GEOSYNTHETICS performed preliminary test and the test results are shown in Table 2.1. The innovative geotextile could transport water to a distance of 72 inches (within 16.5 hours) with zero gradient in drainage test (as shown in Figure 2.10(a)) and wick water to a height of 10 inches (within 2 hours) during capillary rise test (Figure 2.10(b)). The horizontal and vertical wicking tests were conducted under room temperature with relative humidity smaller than 40%, which indicates that the geotextile successfully transport water under unsaturated conditions. Horizontal wicking test proved that the geotextile can transport water without hydraulic gradient and vertical wicking test further validated that capillary force was greater than gravity and could suck water to a depth of 10 inches. Both of the tests didn't count for the amount of water evaporated and it is expected the actual wicking distance or height should be longer and higher than the tested results.

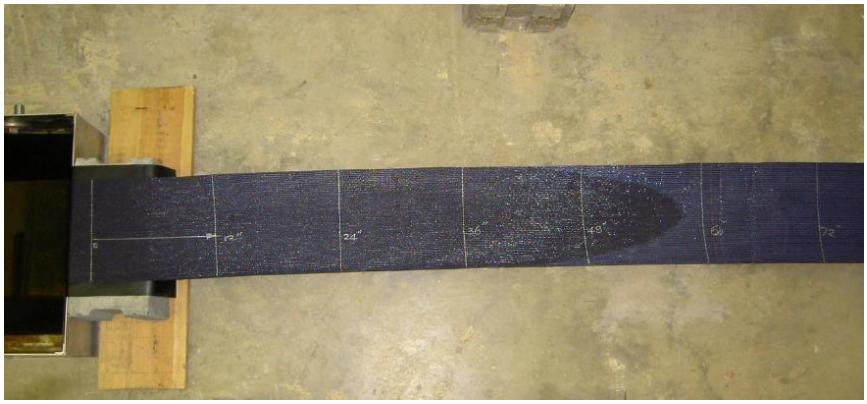

(a) Horizontal Wicking Length Test

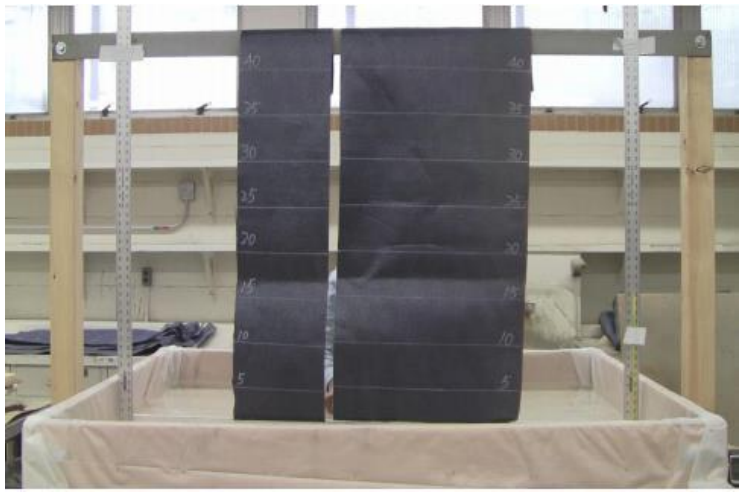

(b) Vertical Wicking Height Test

Figure 2.10 Wetting Front Movement Tests

Researches at University of Alaska Fairbanks (Zhang and Presler, 2012) also conducted a series of tests, including drainage test, capillary rise test, rainfall infiltration test and frost heave test, to evaluate the effectiveness of this geotextile in controlling frost heave issue. For the drainage test, similar results were found that vertical wicking height was 12 inches, which was slightly different from TENCATE's results. The variation might come from several sources such as temperature, relative humidity, testing geotextile width. As for rainfall infiltration test, the test apparatus is shown in Figure 2.11. Four different types of geotextiles were adopted in the rainfall infiltration test, including a wicking fabric, a high performance (HP) reinforcement geosynthetic, a geotextile water filter, and a drainage composite. The tested soil was first saturated and compacted within a plastic mold. Then the mold was put upside down on a layer of geotextile with an impermeable membrane beneath it. The water was allowed to flow for 3 days. Test results indicated that conventional geosynthetics ceased to transport water within 1 day. This phenomenon could be explained the relatively low geosynthetics' air entry values. Due to larger pore geosynthetic pore size, air could easily block the voids under small suction value. Air bubbles were considered similar as soil solids, which were impermeable for water to flow. However, the atmospheric suction value could be as large as 140 MPa and the geosynthetics could be dried very fast under room temperature and relative humidity. Therefore, within limited time period, the geosynthetics ceased to transport water and the tested soils would have larger final water content. In contrast, the geotextile with wicking fabric had large surface area and large air entry value, which enabled the geotextile to wick water out of the soil under higher

suction value and resulted in a lower final water content, as shown in Figure 2.12. Test results of the four different types of geotextile further confirm the fact that the geotextile has advantages to wick water out of soil under unsaturated conditions.

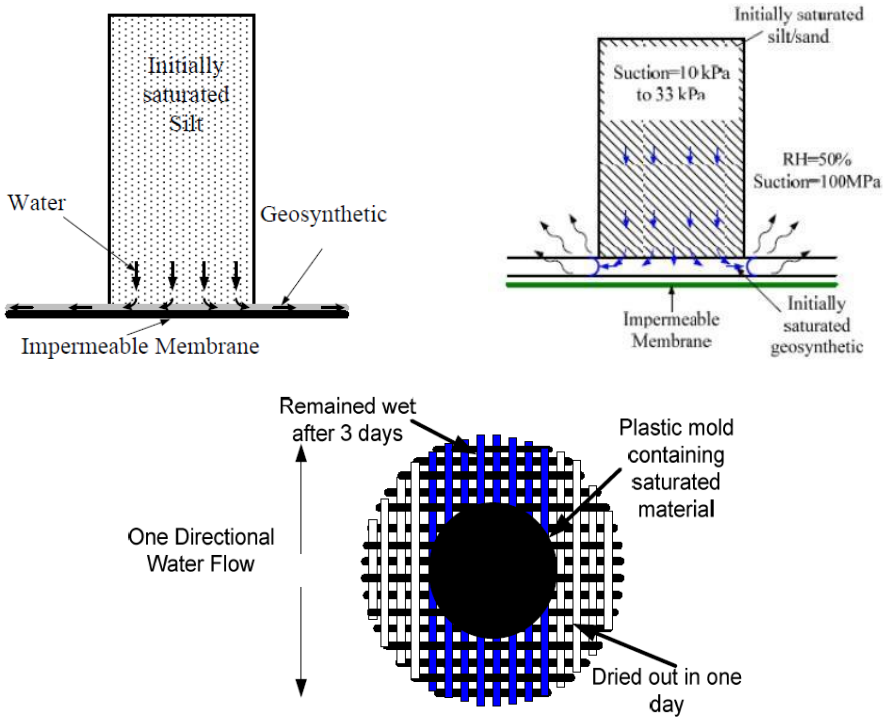

Figure 2.11 Schematic Plots of Rainfall Infiltration Test

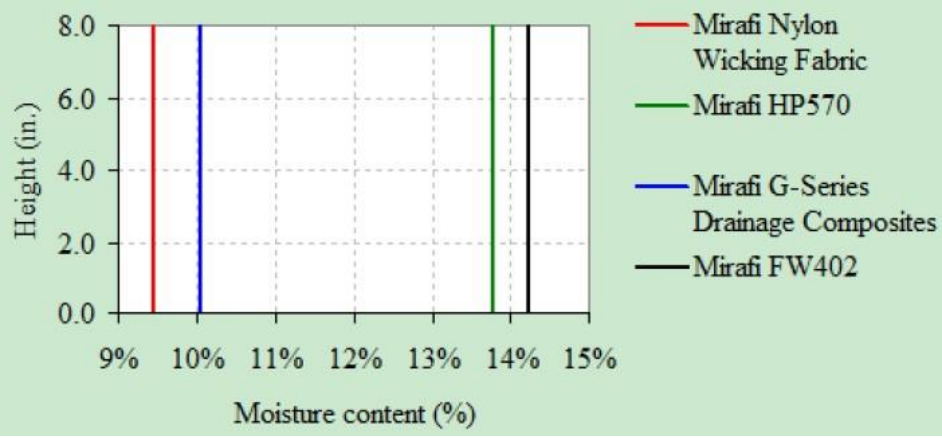

Figure 2.12 Rainfall Infiltration Test Results

Moreover, Wang (Wang et al., 2015) also evaluated the effectiveness of geotextile wicking ability under unsaturated and rainfall conditions. In order to simulate field condition, a layer of the innovative geotextile was sandwiched by a 152 mm thick AB3 subgrade and a 381 mm thick subgrade that mixed with Kansas River sand and Kaolinite. The geotextile extended out of the

closed system to the dehumidifier section so that water could be wicked out. A total amount of 11.3 kg water was poured into the system in order to simulate a 38.1 mm/hour rainfall and the water contents with depths were monitored. Test results indicated that the geotextile effectively wicked water out of soils compacted at optimum moisture content and the water wicked out by the geotextile was 1.65 times greater than that by gravity. Therefore, lab test results provide confident evidence that this type of geotextile has the potential to wick water out of soils under unsaturated conditions and is competitive compared with other types of geotextiles.

2.7 Case Studies of Geotextile with Wicking Ability

Although both laboratory test results indicated that the H2Ri is a very promising drainage material to wick water out of pavement structure, there was no direct evidence to prove any good geotextile field performance. In addition, there were some concerns if the innovative geotextile would be blocked by smaller soil particles and any mechanical punctuation would cause malfunction. Besides the lab level tests, several reports and papers were found regarding the wicking performance of the innovative geotextile as discussed below.

Case 1: Beaver Slide, AK

Zhang (Zhang et al., 2014) reported successful application for the innovative geotextile to prevent frost boils in Alaska pavements. This project located at a section of Dalton Highway, named as “Beaver Slide”, which was unpaved and suffered significant heavy truck traffic. Frost heave and thaw weakening caused extensive damages to the pavement structures. Previous rehabilitation with geocomposite has been proved unsuccessful. In total 22 TDR sensors were used to monitor the temperature and water content change of a 60 ft. long road section the most soft spot, as shown in Figure 2.13. Sieve analysis results indicated that some soils had fine content larger than 6%, which considered as Frost Susceptible (FS) soils. Two layers of innovative geotextile were installed 45 cm apart with the bottom geotextile. Besides temperature and water content sensors inside the test section, other useful data such as air temperature and relative humidity was also recorded for over 2 years.

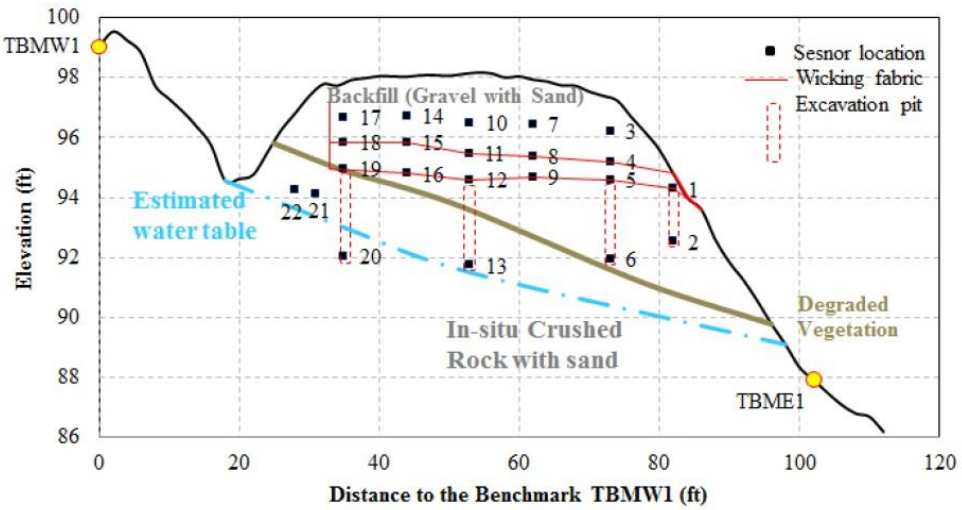

Figure 2.13 Schematic Plot of Test Section

Performances of the geotextile were monitored under different climate conditions, such as rainfall event, freezing process and thawing process. During a rainfall event (Figure 2.14(a)), the water penetrated to a depth of 3 ft below the road surface. The drying process proceeded from east to west, which was exactly the geotextile drainage direction. A drier zone between the two geotextile layers also indicated that the geotextile had larger permeability than the surrounding unsaturated soils and enabled faster drainage process. For freezing process (Figure 2.14(b)), the freezing front penetrated to a depth of 6.5 ft. at the beginning of Nov. 2010 and then continued to move downward to the bottom of the roadway. The unfrozen water content was smaller than 10% after the roadway was completely frozen. As for the thawing process (Figure 2.14(c)), even though it was expected the water content would increase, the soil did not reach saturation and the thawing process didn't started until early spring. It is worthwhile to draw the conclusion that thaw weakening is caused by the thawing of in situ water in the soil.

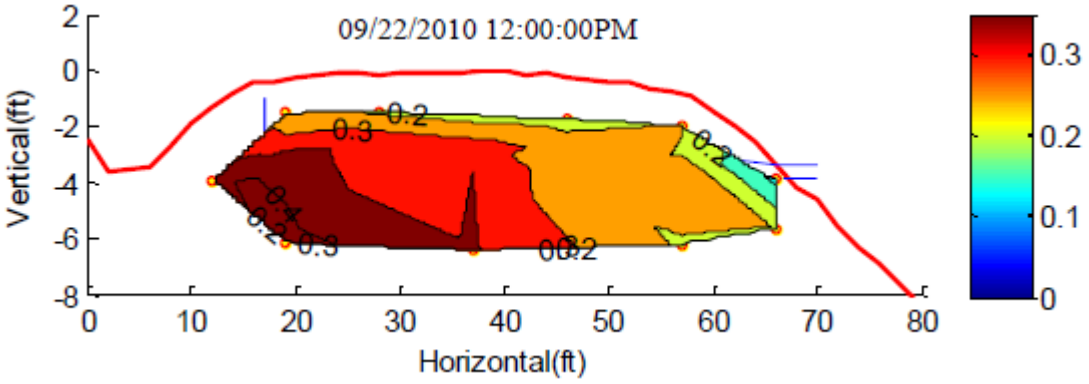

(a) Rainfall Event

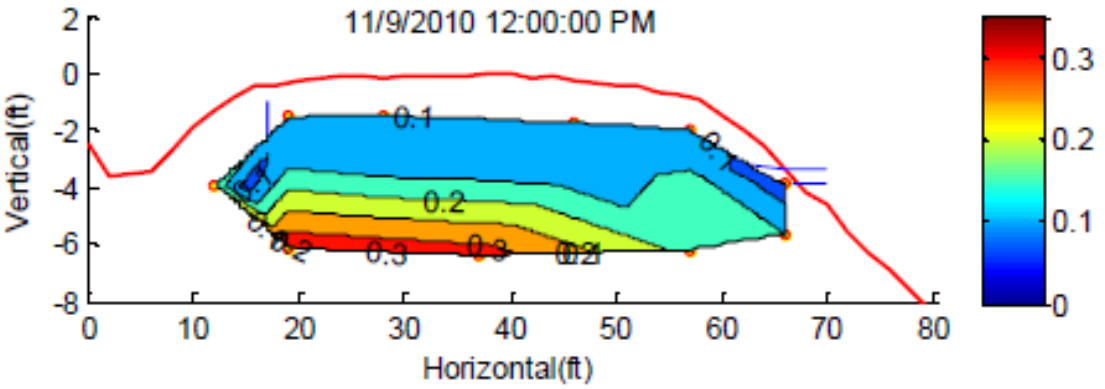

(b) Freezing Process

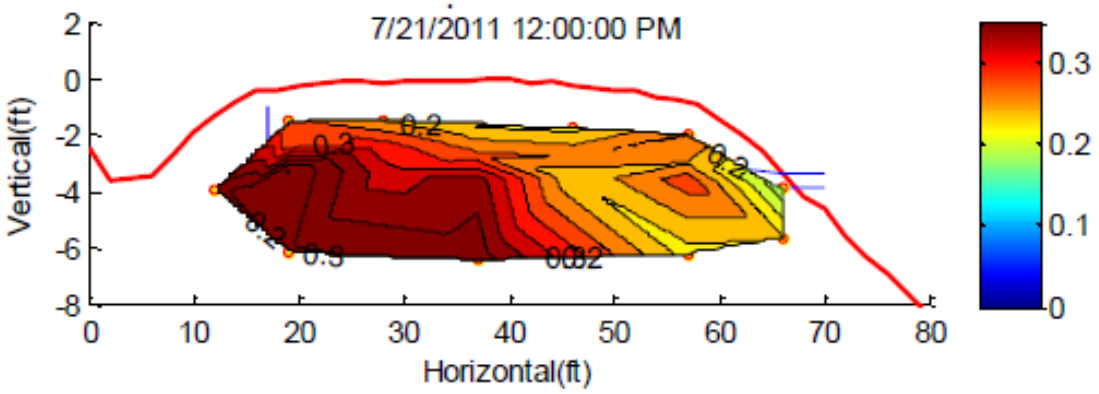

(c) Thawing Process

Figure 2.14 Moisture Contours in Test Section

In a summary, over 2 years of monitoring shows good overall performance for the testing section. Field observation showed a clear road surface difference for sections with and without geotextile, as shown in Figure 2.15. No soft spot was observed during early springs and soil at shoulder was damp, which indicated that water flowed along the direction of the geotextile wicking fabric. The geotextile successfully eliminated the frost and thaw weakening to a depth of 3.5 ft. This could be considered as the effective depth or functional range of the geotextile wickability. Even though soil 4.5 ft. beneath the surface and lower showed the existence of excess water, it was beyond the frost heave and thaw weakening affecting depth and had limited effect on roadway performance.

Figure 2.15 Test Section Comparison

Case 2: Coldfoot, AK

Similar frost heave problems also occurred at harsh environment that located at about 30 miles north of Coldfoot, AK. The road experienced extreme cold temperature and the adjacent ice-rich soil made the frost heave problem even worse. A 12 mile test section (6 mile with geotextile and 6 mile without) was constructed in 2012, which aimed at mitigating the frost heave issue and preventing ice lens formation. 12 inches of aggregate over the geotextile was completed by one lane first. Then the other lane was constructed using the same structure with a minimum of 1.5 ft. geotextile overlap. Test results also showed successful application for geotextile to break water from rising up to the subgrade via capillary action. Since this project was newly operated, close monitoring is required to further evaluate the overall roadway performance for the long-term.

However, as shown in Figure 2.15, preliminary observation already proved the geotextile effectiveness served as a capillary break to wick water out of the pavement structure.

Figure 2.16 Preliminary Field Observation at Coldfoot, AK

Case 3: St. Louis County, MO

A new bridge was being constructed over the Missouri River. The objective of using the geotextile was to remove water from underneath the pavement section. The original design was to construct a pavement section with 4 inches of base aggregate, 4 inches of drainable aggregate and a prepared subgrade. It was expected that the geotextile could reduce the aggregate base material by 2 inches, and also be able to wick water from under the pavement. Observation was shown in Figure 2.16 and the results proved that the geotextile successfully wicked the water out of the aggregate.

Figure 2.17 Field Observation at St. Louis County, MO

Case 4: Texas County, TX

Zornberg (Zornberg et al., 2013) also discussed several cases involving the innovative geotextile in pavement construction and rehabilitation projects. One of the applications was the Texas State Highway 21 rehabilitation project to control different settlement in expansive clay subgrades. The testing area included 8 sections with 4 different types of separator geotextiles, as shown in Figure 2.17. Unfortunately, no conclusive results indicated the effectiveness of the innovative geotextile to change the water content in subgrades. This might because of the high plasticity of the subgrade soil (Plasticity Index = 35%). Another case mentioned in this paper is in Lecheria, Mexico where a pavement section was constructed over a high plasticity clay embankment. A wicking fabric geotextile was used in this project to reduce differential settlement of the plastic clay by balancing non-uniform distribution of moisture, and to reinforce the base course of the road section. Wicking fabric geotextile was placed on top of the subgrade soil to reduce water vertical flow and dissipate water in horizontal direction. The geotextile was also designed to reinforce the base layer, so that the thickness of the base layer would be a minimum of 38 cm (15 inches). The performance of these sections is currently being monitored.

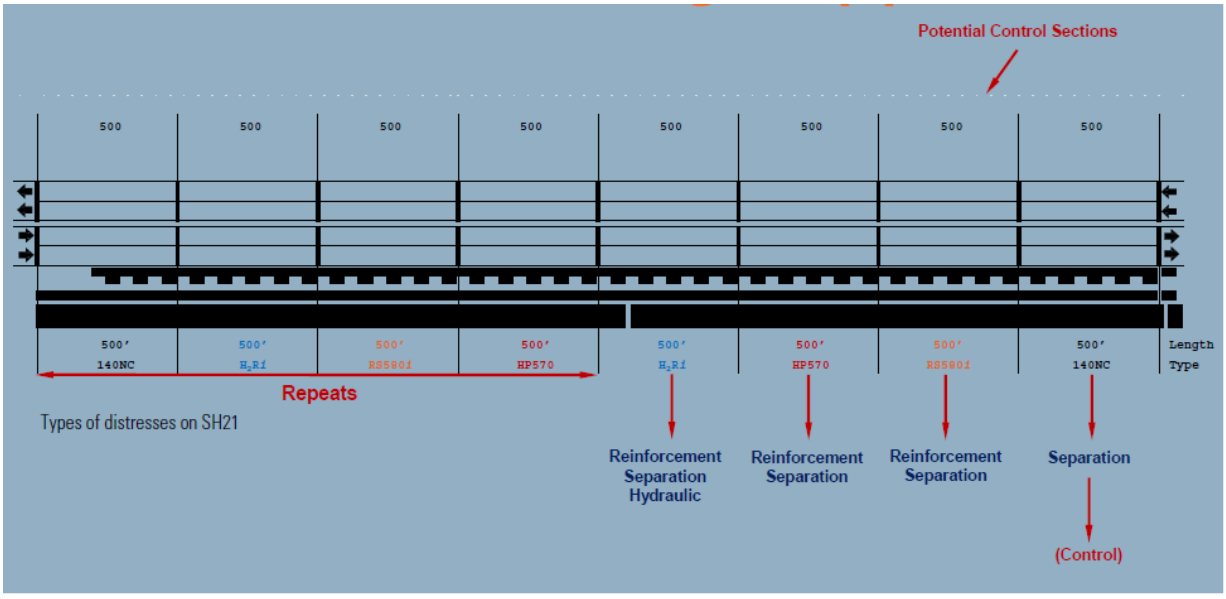

Figure 2.18 Schematic Plot of Test Section at Texas County, TX

Case 5: Corona, CA

In Corona, CA, a large section of roadway was experiencing an excessive amount of natural water run-off, which made the roadway section become saturated and ultimately fail. The geotextile with wicking fabric was provided to help drain away the excess water while providing enhanced stabilization. A 6-inch layer of base material was placed on top of the geotextile. Then, a layer of geogrid was placed on top followed by another 6-inch of base material. A 4-inch layer of AC was the final element of design to complete the road section. Observation indicated that the geotextile provided superior tensile strength at low strain for subgrade support, separated the natural subgrade soils from the aggregate base, wicked excess water, and provided lateral confinement for base section.

Figure 2.19 Field Construction at Corona, CA

Case 6: Jefferson County, WI

Another application occurred at Jefferson County, WI, and the geotextile was used to solve differential settlement problem. The primary challenge was the presence of wet and saturated silt and peat deposits to depths exceeding 30 feet below the existing pavement. Simply removing the deposits is not an economically feasible solution. The geotextile was directly placed on the exposed subgrade, followed by a 15-inch lift of crushed stone, a single layer of geogrid, and a 15-inch lift of crushed stone, as shown in Figure 2.19. Jefferson County Highway Department reported that subgrade undercutting was minimized to 30 inches, compared to a potential 5-8 feet undercut (or more) for the soil conditions present. In addition to the cost savings there was also a substantial time savings in the project construction schedule.

Figure 2.20 Field Construction at Jefferson County, WI

2.8 Potential Issues

Although laboratory and field test results indicated the application of the wicking fabric wass very promising, there are still some concerns regarding use of the wicking fabric for more general conditions. After all, the overall performance of geosynthetic-reinforced pavement structure is dependent upon not only the geosynthetic, but also the soil and soil – geotextile interaction. Before extensive engineering applications of this type of geotextile, there are several issues need to be answered. For example, can this application be extended to other types of soils? To what extent can the pavement structure water content be reduced? By implementing this type of wicking fabric, how much improvement can be obtained for the pavement structure in terms of resilient modulus, permanent deformation, and shear strength along the soil-wicking geosynthetic interface? Most importantly, the wicking fabric will stop working? If yes, at what condition.

Besides the discussions above, there are some other concerns regarding the geotextile applications. Figure 2.20 shows the Scanning Electron Microscope (SEM) images of the samples that collected from the field. Left figure shows the SEM image of the wicking fabric at the surface of the woven geotextile. The "clogging effect" was defined as the phenomena that (1) magnitude of confining pressure in soil on drainage path, (2) physical disturbance on drainage path, (3) air bubbles stuck into drainage path, and (4) permeability influenced by the intrusion of fine particles (Palmeria and Gardoni, 2000). Observed results indicate that all the surface edges of the wicking fabric were suffered from clogging effect. Since the soil above the

geotextile was consolidated, the soil thoroughly blocked the wicking path (detained on the deep grooves) and impeded the drainage efficiency. However, in contrast, figure on the right side was the SEM images of wicking fabrics beneath the surface. The drainage paths were clean and very limited amount of soil particles were detained within the drainage paths. Therefore, clogging effect only occurred at the geotextile surface, and its effect on geotextile performance still need to be further investigated. One recommendation to minimize the clogging effect might be twisting the wicking fabric yarn during fabrication process to reduce the surface exposed to the soil.

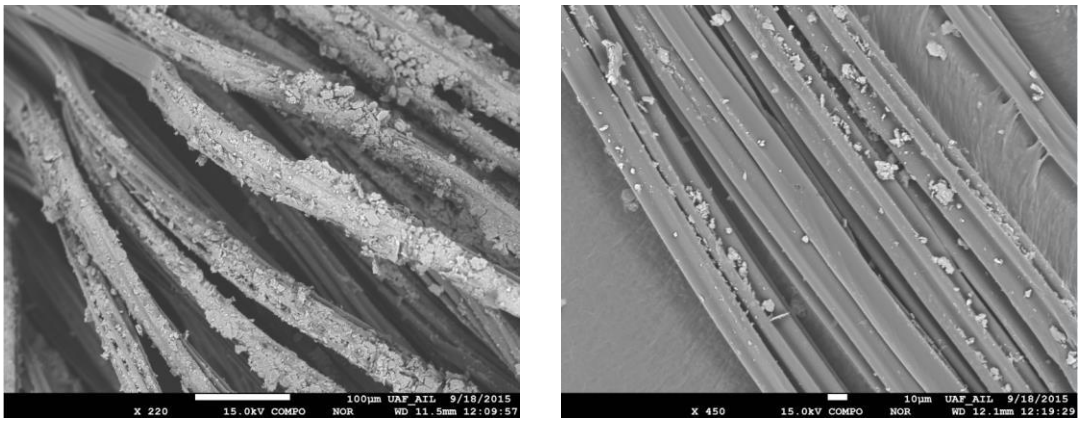

(a) (b)

Figure 2.21 Clogging Effect SEM Images

Figure 2.21 shows another potential wicking fabric failure due to high vertical pressure. The woven part of the fabric was compressed and the wicking paths were all squeezed together. Figure 2.21(a) shows the fabric yarn without disturbance. Again, all the surface layer that exposed to the soil suffered from clogging while the overlapped wicking fabrics was mechanically compressed due to higher vertical pressure. A closer top view of the compressed area is shown in Figure 2.21 (b). The drainage paths were flattened and might not hold and transport water through the grooves. Even though no soil particles were detained here, the deep groove may fail to work under unsaturated conditions and the draining efficiency would be compromised. Figure 2.21 (c) and (d) show the compressed area from different angles. Since vertical pressure was much larger than confining pressure, the deep grooves were only compressed in one direction, which means the grooves in confining direction might still work.

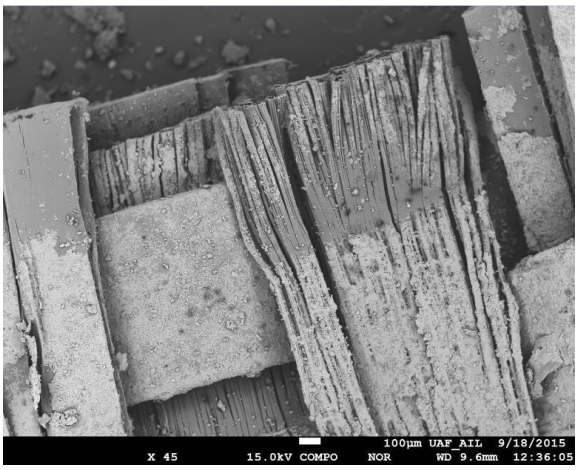

(a)

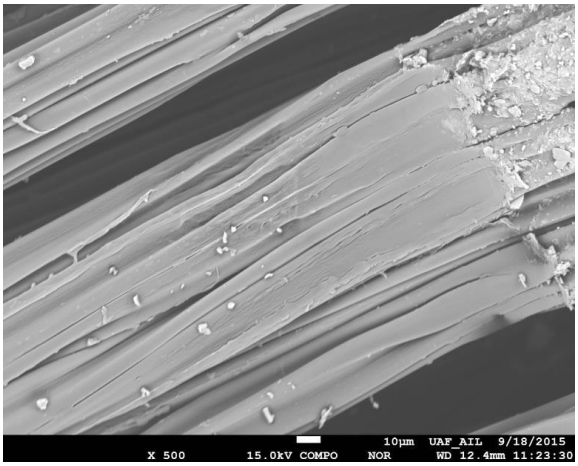

(b)

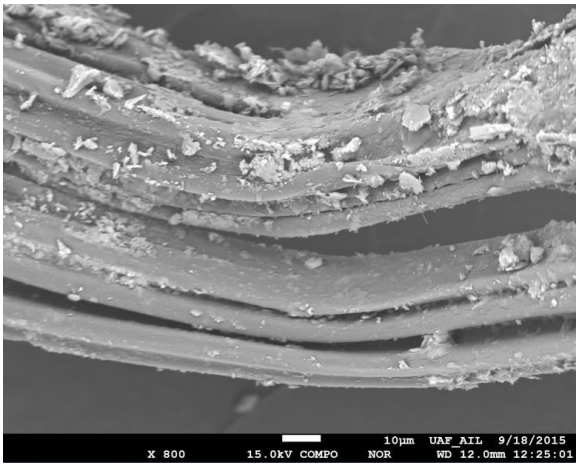

(c)

(d)

Figure 2.22 Mechanical Failure SEM Images

Figure 2.22 shows the wicking fabric failure due to punctuation. Although the wicking fabric has higher strength, punctuation failure under high pressure would cause the worst scenario

since the deep grooves were entirely broken off and the drainage paths were thoroughly discontinued.

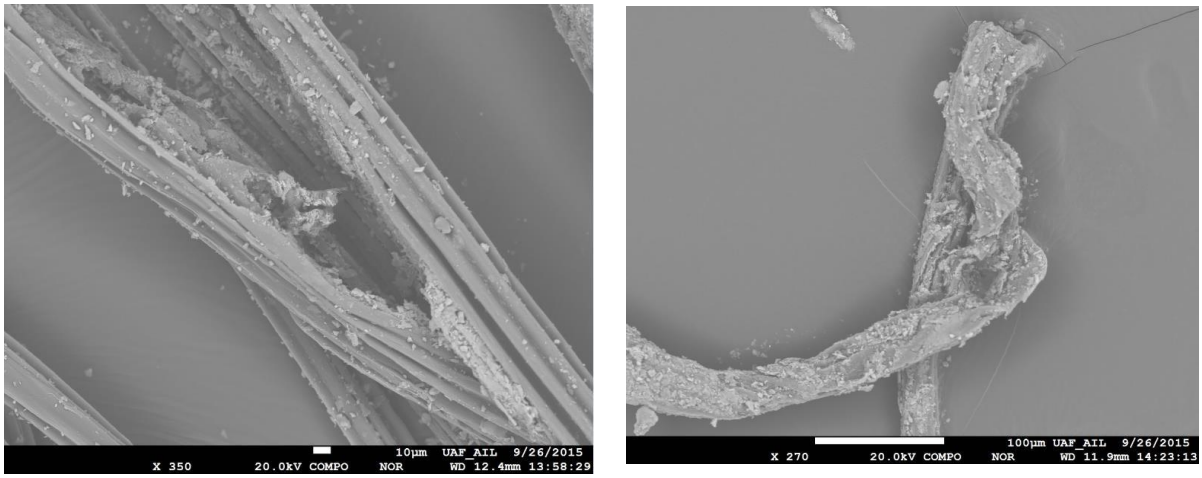

(a) (b)

Figure 2.23 SEM Images of Punctuation Failure

2.9 Reference

Han, J. and Zhang, X. (2014). "Recent Advances in the Use of Geosynthetics to Enhance Sustainability of Roadways." *20th International Conference on Advances in Civil Engineering for Sustainable Development*, Suranaree University of Technology, Nakhon Ratchasima, Thailand, pp. 29-39.

Taylor, M. A. and Khosla, N. P. (1983). "Stripping of Asphalt Pavement-State of the Art." In Transportation Research Record 911, *TRB National Research Council*, Washington, D.C., pp. 150-158.

Mallela, J. L., TiTus-Glover and Darter, M. I. (2000). "Considerations for Providing Subsurface Drainage in Jionted Concrete Pavements." In Transportation Research Record 1709, *TRB National Research Council*, Washington, D.C., pp. 1-10.

Chamberlain, E. J. (1987). "A Freeze-Thaw Test to Determine the Frost Susceptibility of Soils." *U. S. Army Corps of Engineers, Cold Regions Research and Engineering Laboratory (CRREL),* Special Report: 87-1.

Casagrande, A. (1931). "Discussion of Frost Heaving," *Highway Research Board*, Proceedings, Vol. 11, pp. 163-172.

Csathy, T. I. and Townsend, D. L. (1962). "Pore Size and Field Frost Performance of Soils" *Highway Research Board Bulletin*, No.331, pp. 67-80.

Casagrande, A. (1947). "Classification and Identification of Soils." *Proceedings, American Society of Civil Engineers*, Vol. 73(6), pp. 283.

Taber, S. (1930a). "The Mechanics of Frost Heaving." *Journal of Geology*, Vol. 38, pp. 303-317.

Taber, S. (1930b). "Freezing and Thawing of Soils as Factors in the Destruction of Road Pavements." *Public Roads*, Vol. 11(6), pp. 113-132.

Takagi, S. (1978). "Segregation Freezing as the Cause of Suction Force in Ice Lens Formation." *Cold Regions Research and Engineering Laboratory (CRREL),* Report No. 78-6, pp, 12.

Takagi, S. (1980). "The Adsorption Force Theory of Frost Heaving." *Cold Regions Science and Technology,* Vol. 3, pp. 57-81.

Polubarinova-Kochina, and Ya, P. (1952). "Theory of the Motion of Ground Water." Gostekhizdat, Moscow, USSR.

Aravin, V. I. and Numerov, S. N. (1953). "Theory of Fluid Flow in Undeformable Porous Media." Gostekhizdat, Moscow, USSR.

Muskat, M. (1946). “The Flow of Homogeneous Fluids Through Porous Media.” *J. W. Edwards, Publisher,* Ann Arbor, Michigan.

Lane, K. S. and Washburn, D. E. (1946). “Capillary Tests by Capillarimeter and by Soil Filled Tubes.” *Proceedings, Highway Research Board*.

Barber, E. S. and Sawyer, C. L. (1952). “Highway Subdrainage.” *Public Roads*, Vol. 26(12).

Brown, S. A., Stein, S. M., and Warner, J. C. (2001). “Urban Drainage Design Manual, Hydraulic Engineering Circular 22, Second Edition.” *Federal Highway Administration,* Publication No. FHWA-NHI-01-021.

Cedergren, H. R. (1974). “Drainage of Highway and Airfield Pavements.” *John Wiley and Sons*, New York.

Cedergren, H. R., Arman, J. A., and O'Brien, K. H. (1973). “Development of Guidelines for the Design of Subsurface Drainage Systems for Highway Pavement Structural Sections, Final Report.” *Federal Highway Administration*, Washington, D, C., February, 1973.

MEPDG (2004). “National Cooperative Highway Research program, Transportation Research Board and National Research Council. Mechanistic-Empirical Design of New and Rehabilitated Pavement Structures.” *National Cooperative Highway Research Program*, NCHRP Project 1-37A Report, National Research Council. Washington, DC.

FHWA (1980). “Highway Subdrainage Design. Publication.” *Federal Highway Administration (FHWA)*, FHWA-TS-80-224, U.S. Department of Transportation.

AASHTO (1993). “AASHTO Guide for Design of Pavement Structures.” *American Association of State Highway and Transportation Officials (AASHTO),* Washington D. C., USA.

Rutledge, P. C. and Johnson, S. J. (1958). “Review of Uses of Vertical Sand Drains.” Bulletin 173, *Highway Research Board,* Wahsington, D. C..

Rechart, F. E. (1957). “Review of the Theories for Sand Drains.” Transactions, *American Society of Civil Engineers*, Vol. 124.

Anderson, D. A., Huebner, R. S., Reed, J. R., Warner, J. C., and Henry, J. J. (1998). “Improved Surface Drainage of Pavements.” *National Cooperative Highway Research Program (NCHRP)*, Project No. 1-29.

Fredlund, D. G. and Rahardjo, H. (1993). “Soil Mechanics for Unsaturated Soils.” *John Wiley & Sons.*

Zhang, X. and Presler, W. (2012). "Use of H2Ri Wicking Fabric to Prevent Frost Boils in the Dalton Highway Beaver Slide Area, Alaska." *Alaska University Transportation Center (AUTC) Project Report*, No. RR10.02 & 510020, August, 2012.

Wang, F., Han, J., Zhang, X., and Guo, J. (2015). "Laboratory Test to Evaluate Effectiveness of Wicking Fabric in Soil Moisture Reduction." *Journal of Geotechnical and Geoenvironmental Engineering*, ASCE. (Under Review)

Zhang, X., Presler, W., Li, L., Jones, D. and Odgers, B. (2014). "Use of Wicking Fabric to Help Prevent Frost Boils in Alaskan Pavements." *Journal of Materials in Civil Engineering*, ASCE, pp 739.

Zornberg, J. G., Odgers, B., Roodi, G. H., and Azevedo, M. M. (2013). "Advantages and Applications of Enhanced Lateral Drainage in Pavement Systems." *Proceedings of the 2nd African Regional Conference on Geosynthetics*, GeoAfrica 2013, 18-20 November, Accra, Ghana, pp. 539-548.

Palmeria, E. M. and Gardoni, M. G. (2000). "Influence of Partial Clogging and Pressure on the Behavior of Geotextiles in Drainage System." *Geosynthetics International*, Vol. 7, pp. 403-431.

CHAPTER 3 TESTING FLUME SETUP

Two test flumes were constructed to evaluate the wicking effect of the fabric. One flume was filled with sand, and the other one was filled with Fairbanks silt (contains about 5% organic material). The schematic plot of the testing flume is shown in Figure 3.1. The dimensions for the testing flumes were 252 in. × 16 in. ×12 in. (Length × Width × Height). Three layers of sensors located at depths of 1 in., 5 in. and 9 in. from the bottom to the top. The wicking fabric was located at 1 in. from the bottom of the testing flume. The left side of the fabric was exposed to the open air. A 3 ft. long overlap wicking fabric started at 5 ft. from the left side of the testing flume. For the testing flume with sand, two types of sensors were used: MPS-2 water potential sensor to measure the soil suction and EC-5 moisture sensor to measure the moisture content.

The moisture content sensors were marked numerically and the water potential sensors were marked alphabetically. Yet, since the water potential sensors did not work effectively, only the moisture sensors were used for testing flumes for silt.

The construction process started by filling the flume with 1 in. of saturated sand, as shown in Figure 3.2(a). The testing flume was first covered with a layer of plastic wrap to prevent water from flowing outside the system. Both sides of the flume walls were marked at the anticipated heights and the sand was then flattened with a trowel to the marker. After that, the wicking fabric was put into the testing flume as shown in Figure 3.2(b). Since the fabric roll was not long enough, a 3 ft. overlap was placed at a distance of 5 ft. from the left side of the testing flume. Then, the first layer of sensor was place on top of the fabric as shown in Figure 3.2(c). One set of sensors was put at each location and in total 8 sets of sensors in one layer. The fabric was then saturated with water before another layer of soil was put into the testing flume. Figure 3.2(d) shows the testing flume filled with 12 in. of saturated sand. The walls of the testing flume was fastened with wood plates to prevent the walls from expanding. After all the sensors were put into the testing flume, the testing system was covered with plastic wrap as shown in Figure 3.2(e).

Furthermore, at the left side of the testing flume, the wicking fabric was exposed to the open air so that the water inside the testing system could be wicked out.

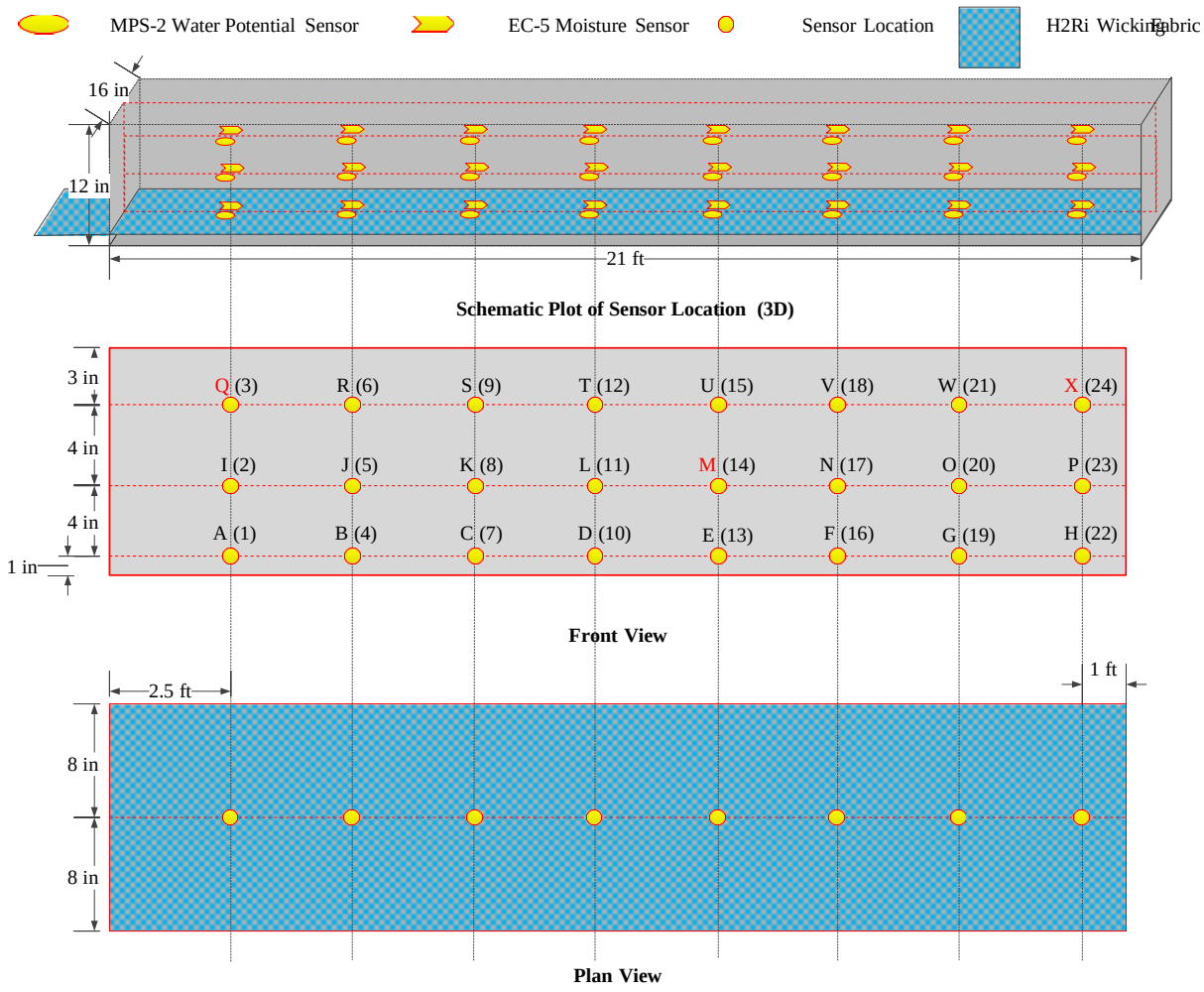

Figure 3.1 Schematic Plot of Testing Flume and Sensor Location

(a) (b)

(c)

(d)

(e)

(f)

Figure 3.2 Testing Flume Construction

Figure 3.3 shows the data acquisition system. The system was composed of 1 CR1000 datalogger and 1 AM 16/32 multiplexer. The CR1000 was used to store the monitored data at a time interval of 1 hour. The AM 16/32 multiplexer provided the pots to connect in total 48 sensors (24 water potential sensors and 24 moisture content sensors).

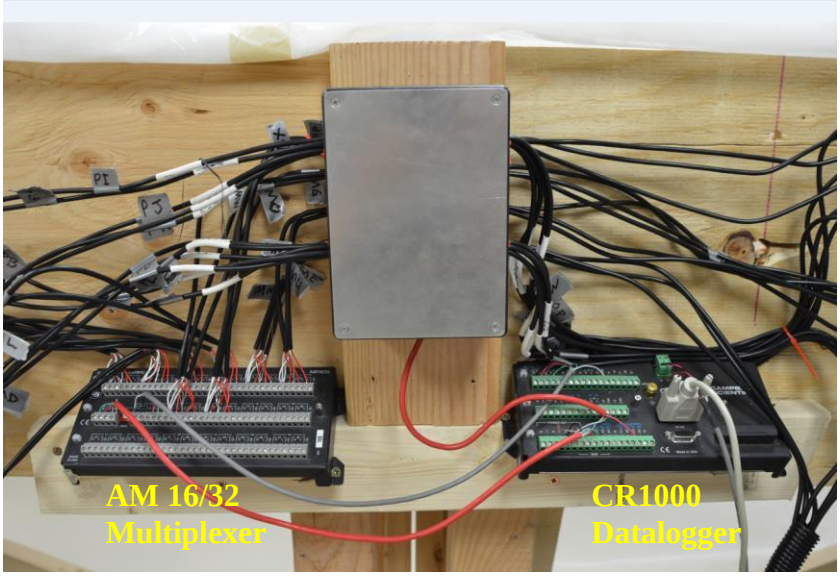

Figure 3.3 Data Acquisition System

CHAPTER 4 TEST RESULTS AND DISCUSSIONS

In general, the test results were categorized into three types of tests, including:

1. Wicking Test: evaluating the effectiveness of the wicking fabric during drying process;
2. Wetting Test: evaluating the effectiveness of the wicking fabric during wetting process;
3. Rewicking Test: assessing the effectiveness of the wicking fabric during cyclic drying-wetting process.

Case 1: Wicking Test for Sand

Wicking test for sand started at 2 pm on September 6, 2014. In this case, the moisture contours for the testing flume were plotted at starting point, 2 hours, 1day, 10 days and 1 month, as shown in Figure 4.1. At the starting point, due to gravitational drainage, the moisture content decreased with increment of vertical height. The moisture content changed from 0.3 at the bottom to 0.22 at the top. Moreover, since there was a 3 ft. wicking fabric overlap between 5 ft. and 8 ft. from the left side of the testing flume, the maximum moisture content occurred at the overlapping area. This indicated that the effectiveness of the wicking fabric dramatically diminished due to poor contact condition. After 2 hours, the moisture content at the top of the flume decreased to about 1.2. The moisture content at left side of the flume decreased than the right side of the flume because the wicking fabric exposed to the open air. After 1 day, the moisture content at the top of the flume further decreased to about 0.15. It is worthwhile to point out that even though the wicking fabric effectively transported the water from the left to right except for the overlapping area. And the effect did not disappear throughout the entire testing period. By looking at the moisture contours after 10 days and 1 month, the moisture content at top of the flume further dropped to about 0.1 and the wicking fabric worked effectively except for the overlapping area.

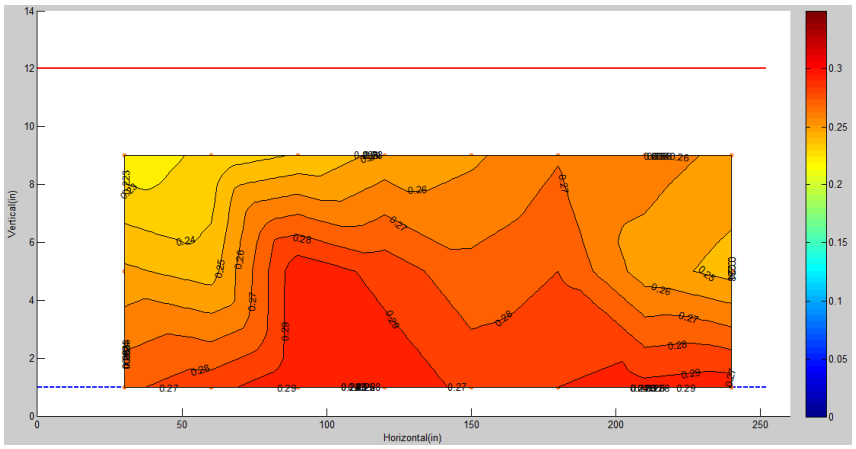

(a) Starting Point

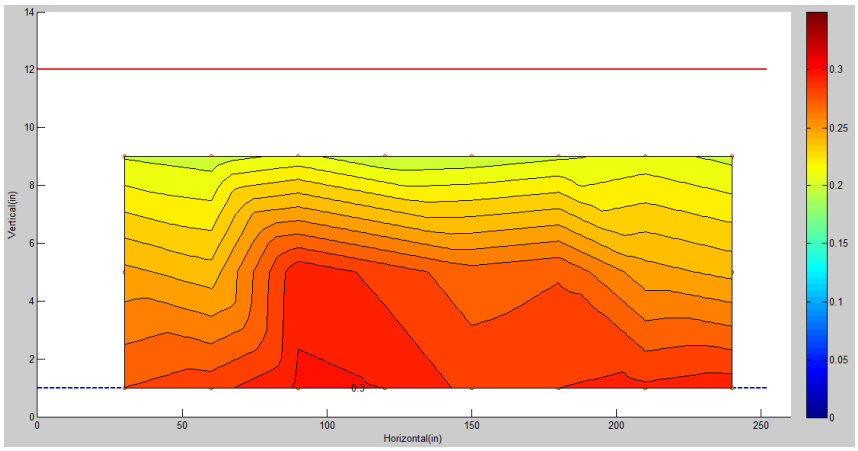

(b) 2 Hours

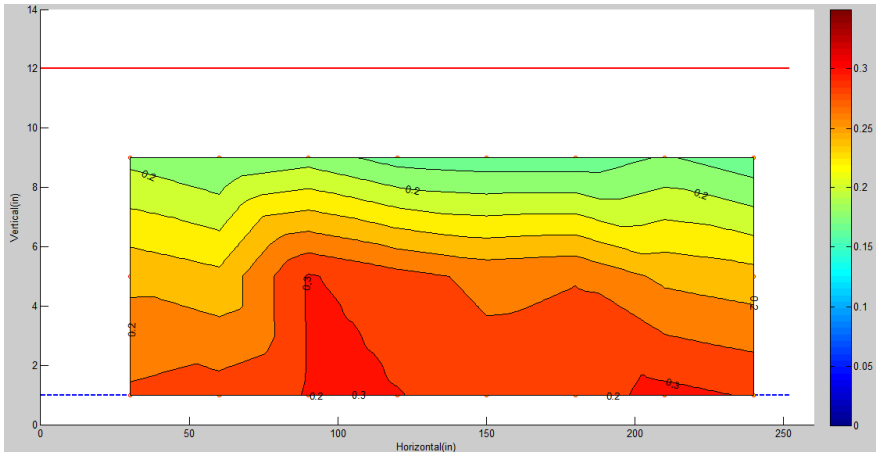

(c)) 1 Day

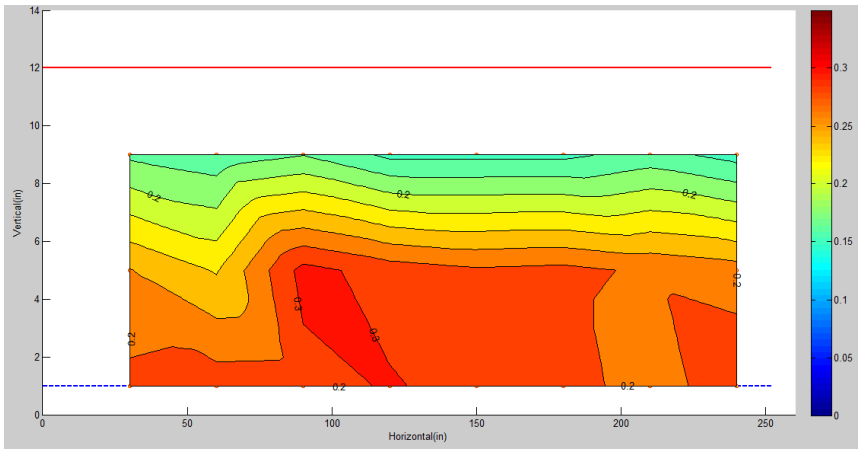

(d) 10 Days

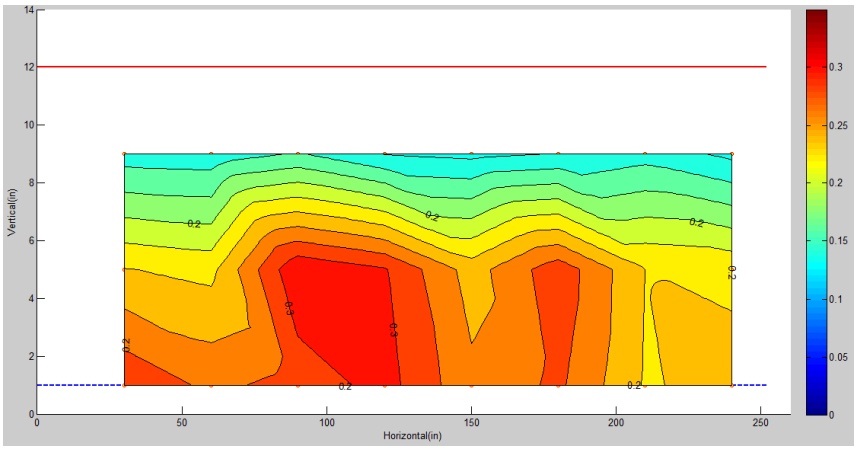

(e)) 1 Month

Figure 4.1 Moisture Contour for Wicking Test (Sand)

Case 2: Wetting Test for Sand

Wetting test for sand started at 5 pm on November 2, 2014. The left side of the fabric was dipped into water rather than exposed to open air. Figure 4.2 shows the moisture contour for the testing flume at starting point, 2 hours, 1 day, 10 days and 1 month. This time, the water flowed from left to right. At the starting point, the moisture content at the left side of the flume increased instantaneously due to the wetting of the fabric. Due to the poor connection at the overlapping area, the water could not transport further to the right side of the flume within 1 day. After 10 days, the accumulated water at the overlapping area transported further to 180 in. The wicking fabric continued to transport water to the right side of the flume and resulted in a slight increment in moisture content by 5% after 1 month. In general, the overlapping of the wicking fabric significantly decreased its wickability to transport the water to the right side of the testing flume.

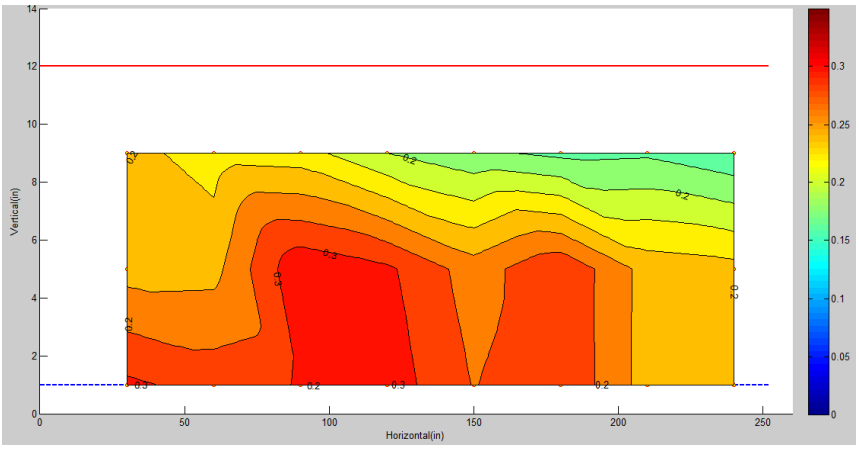

(a) Starting Point

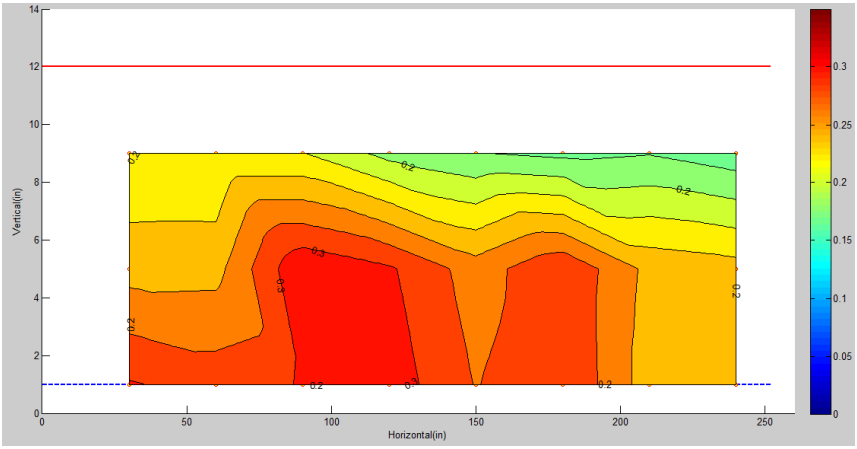

(b) 2 Hours

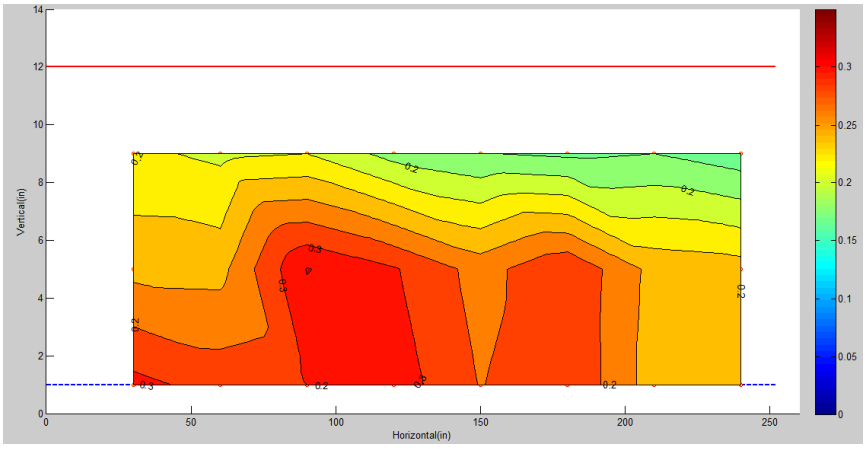

(c)) 1 Day

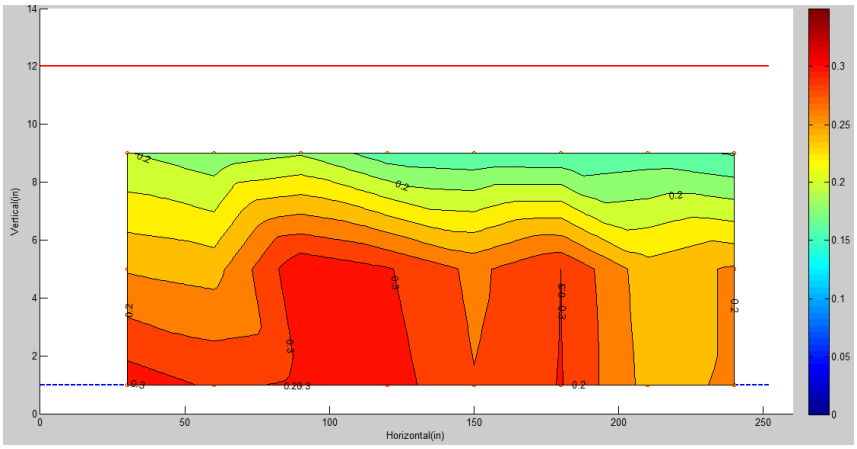

(d) 10 Days

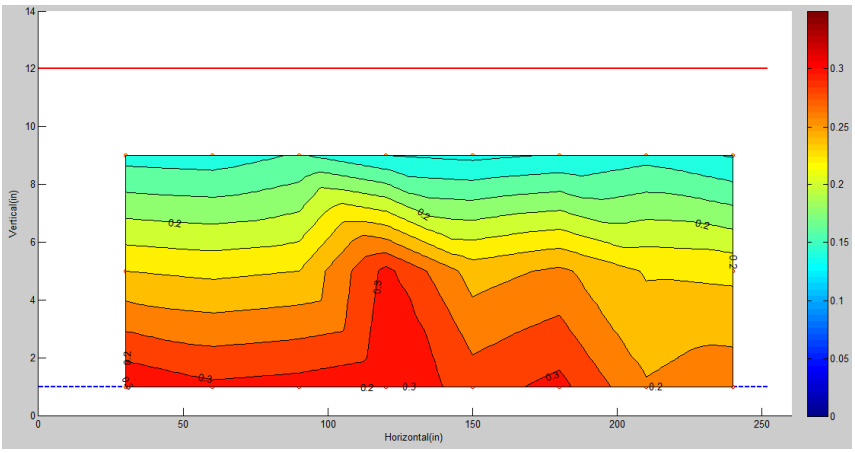

(e)) 1 Month

Figure 4.2 Moisture Contour for Wetting Test (Sand)

Case 3: Rewicking Test for Sand

Rewicking test for sand started at 11 am on March 13, 2015. On the right side of the testing flume, 1 ft. wide of the solid was moved out and a wood board was placed into the flume to prevent the soil from collapsing. In total 10 gallon of water was poured into the gap and the moisture content was monitored. Figure 4.3 shows the moisture contour for the testing flume at starting point, 2 hours, 1 day, 10 days and 1 month. Similar results were observed as for wetting test. The right side of the testing flume increased instantaneously after pouring the water and the water was transported to the overlapping area. After 10 days, the moisture content at the right side of the testing flume decreased dramatically to about 0.21 due to the combination effect of evaporation and wicking. After 1 month, the moisture content kept increasing at the overlapping area, which indicates that the effectiveness of wicking again decreased dramatically due to poor connection.

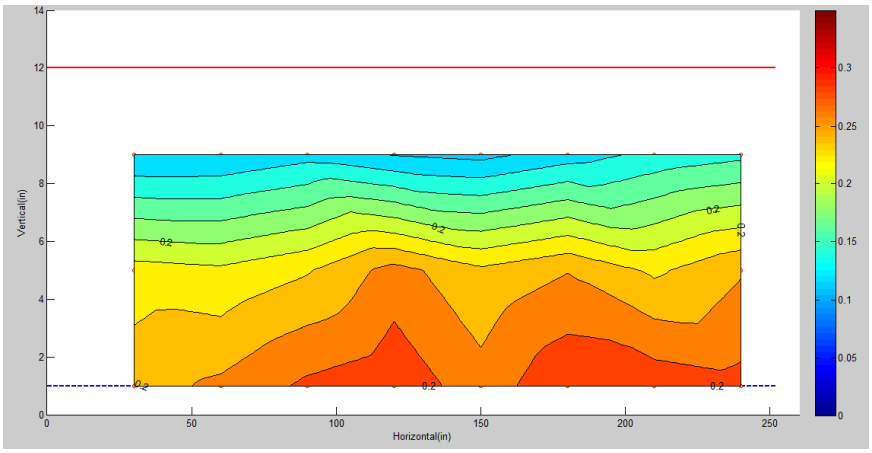

(a) Starting Point

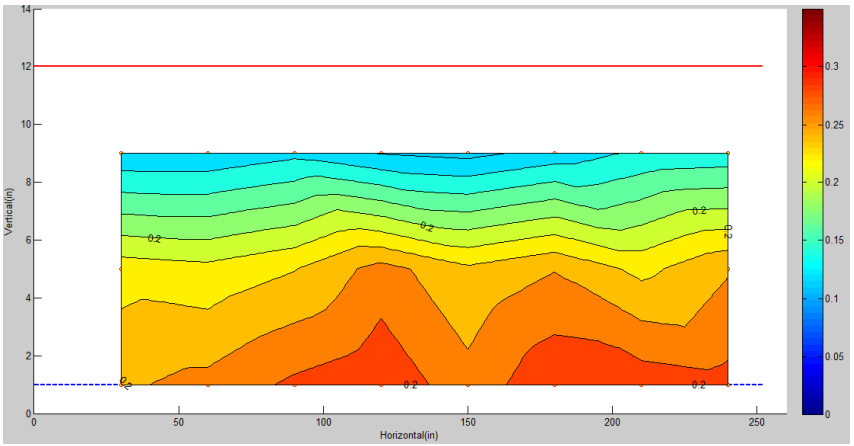

(b) 2 Hours

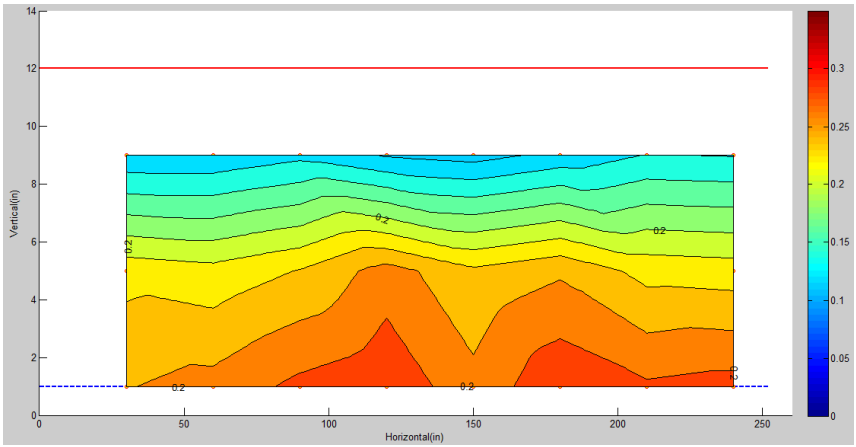

(c)) 1 Day

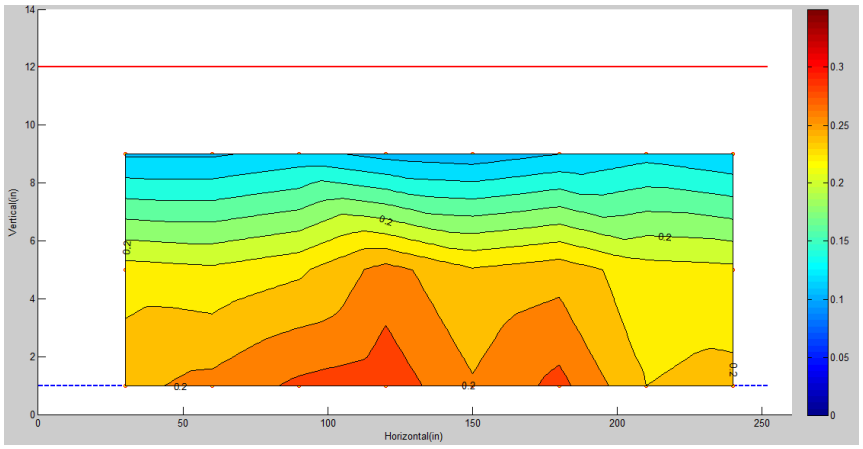

(d) 10 Days

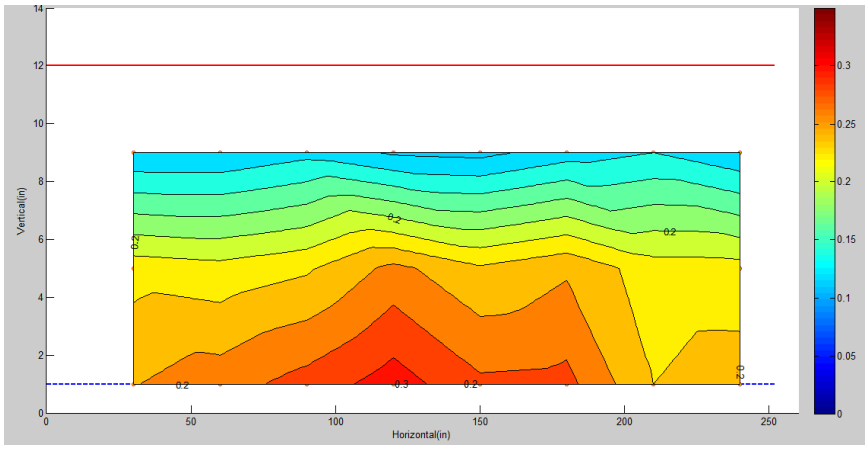

(e)) 1 Month

Figure 4.3 Moisture Contour for Rewicking Test (Sand)

Case 4: Wicking Test for Silt

Wicking test for silt started at 4 pm on December 23, 2014. The moisture content contours are plotted at starting point, 2 hours, 1 day, 10 days and 1 month, as shown in Figure 4.4. At the starting point, the moisture content at the left side of the flume first started to decrease because of the wicking effect. Also, similar to sand, the overlapping area experienced a smaller moisture content decrease due to the poor connection and drainage condition. After 2 hours, the water flowed from right to left and accumulated at the overlapping area resulted in an even larger moisture content at the overlapping area. After 1 day, the blue areas indicated the moisture contents were much smaller than the surrounding area. Several major cracks were observed during the consolidation process and the air could penetrate into the soil through the cracks. Since air circulating would increase the evaporation process, the moisture content decreased faster than those areas without cracks. Thus Figure 4.4(c) is reasonable in explaining the drying procedure described above. After 10 days, the excess water at the overlapping area was gradually wicked out and moisture content decreased to about 2.40. Then after 1 month, the effect of

crackings on the moisture content change was more obvious. The moisture contents at three major cracks (60 in., 147 in. and 192 in.) were much smaller than the surrounding soils.

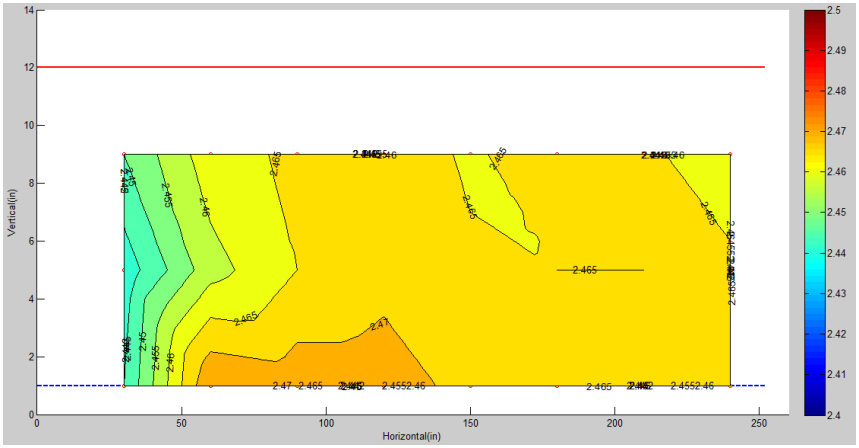

(a) Starting Point

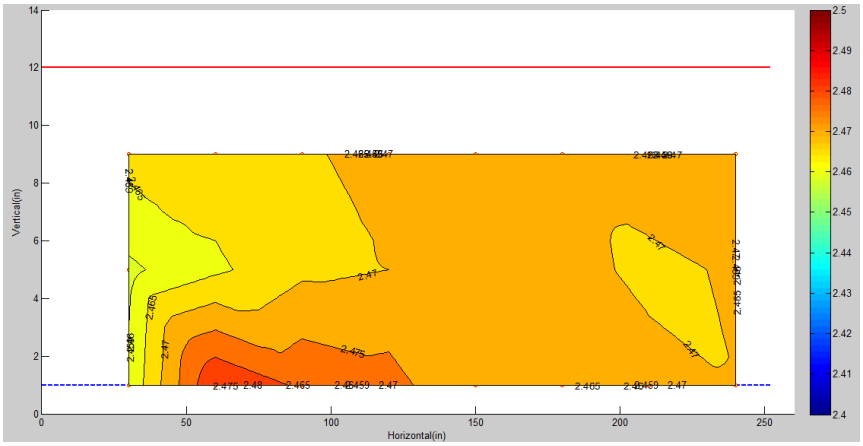

(b) 2 Hours

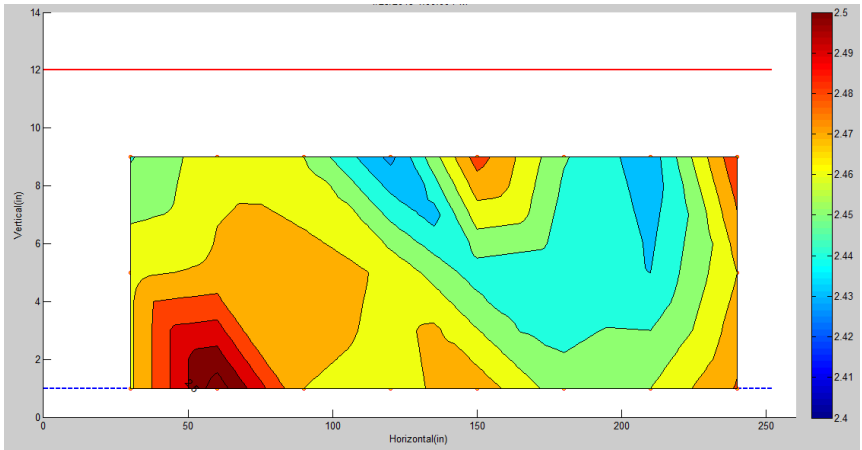

(c)) 1 Day

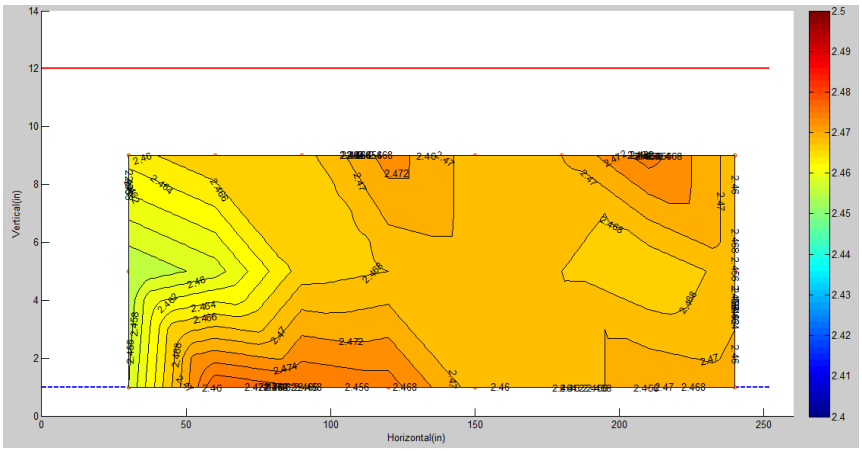

(d) 10 Days

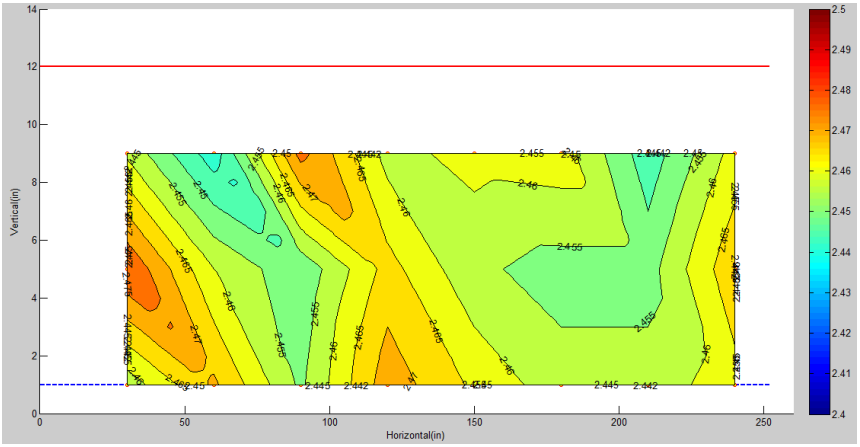

(e)) 1 Month

Figure 4.4 Moisture Contour for Wicking Test (Silt)

Case 5: Rewicking Test for Silt

Rewicking test for silt started at 2 pm on March 12, 2014. The moisture content contours are plotted at starting point, 2 hours, 1 day, 10 days and 1 month, as shown in Figure 4.5. Compared with wicking test, the water flow rate for rewicking test was much smaller. After 1 day, the shape of the moisture contour did not change too much. Two major reasons would cause such phenomenon: 1) the permeability of silt itself is much smaller than that of sand; 2) the wicking paths within the fabric might be detained by the fine particles and thus significantly reduced the water flow rate. After 1 month, the moisture contents near the three major cracks further decreased and the amount of accumulated excess water was much smaller than previous.

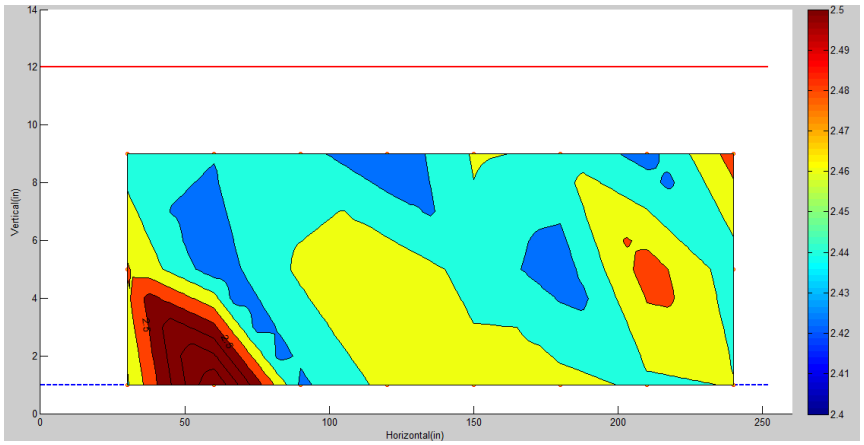

(a) Starting Point

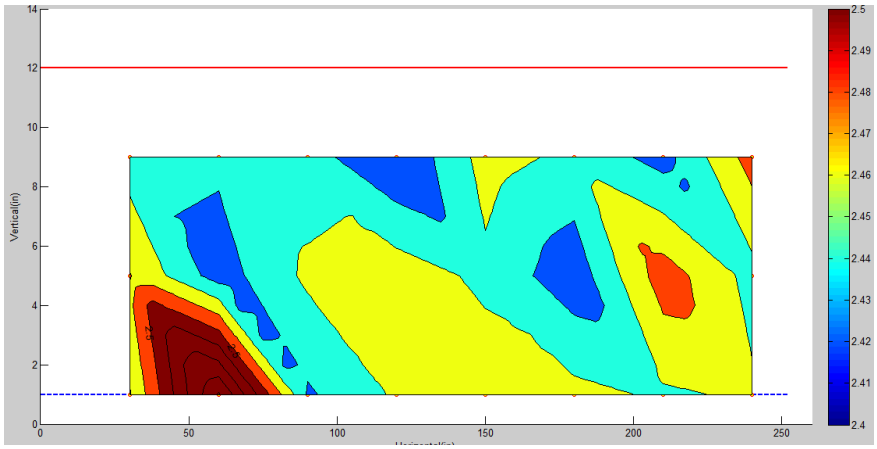

(b) 2 Hours

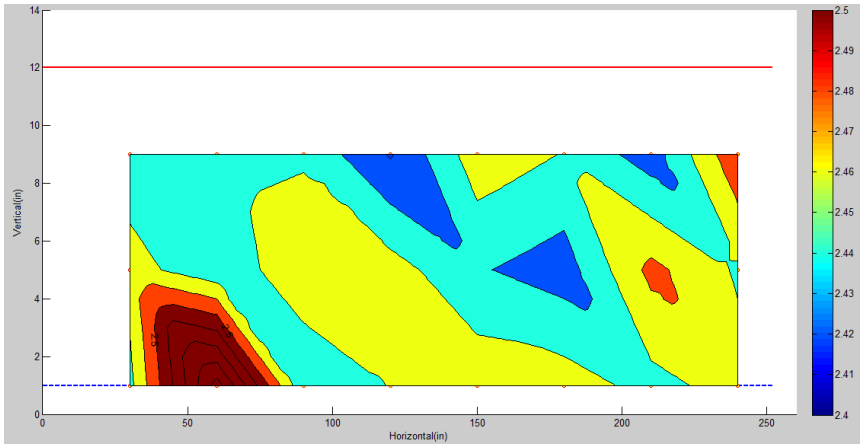

(c)) 1 Day

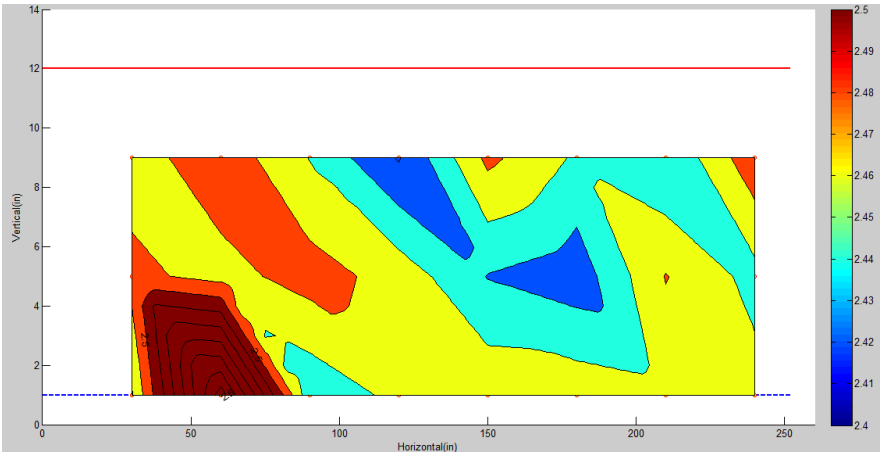

(d) 10 Days

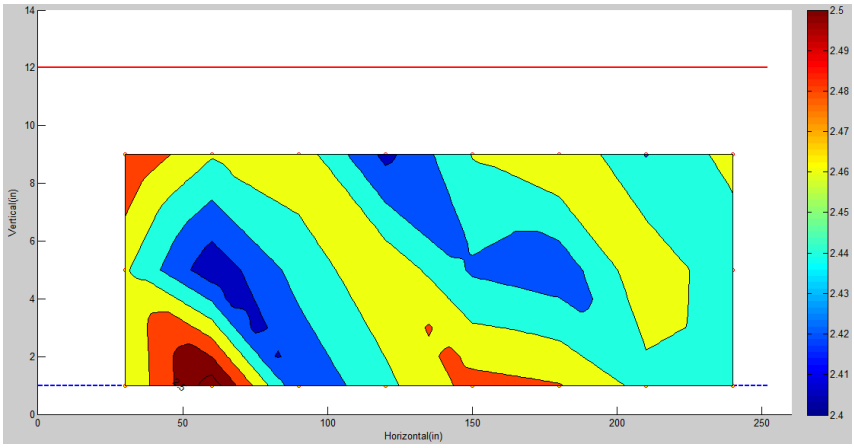

(e)) 1 Month

Figure 4.5 Moisture Contour for Rewicking Test (Silt)

Figure 4.6 Photo of organic silt and blinding of the fabric at the bottom.

It is clear that the organic silt has low permeability. The water added the inlet end of the flume stabilized at about 8 inches and remained essentially at that height. This clearly indicates that the silt is impermeable and that the wicking fabric had failed to transfer water. Photo-micrographs were taken of a bundle of fibers at a magnification of 1500x. Figure 4.6 shows that the fibers were blinded by the small clay particles contained in the silt which rendered the fabric ineffective.

CHAPTER 5 SUMMARY AND CONCLUSIONS

The fabric was immediately blinded and ceased to perform in the flume containing the organic silt. This was confirmed by two methods, first by supplying clear water at the upstream end of the fabric. The fabric failed to remove any of the water. The fabric at the outlet of the flume

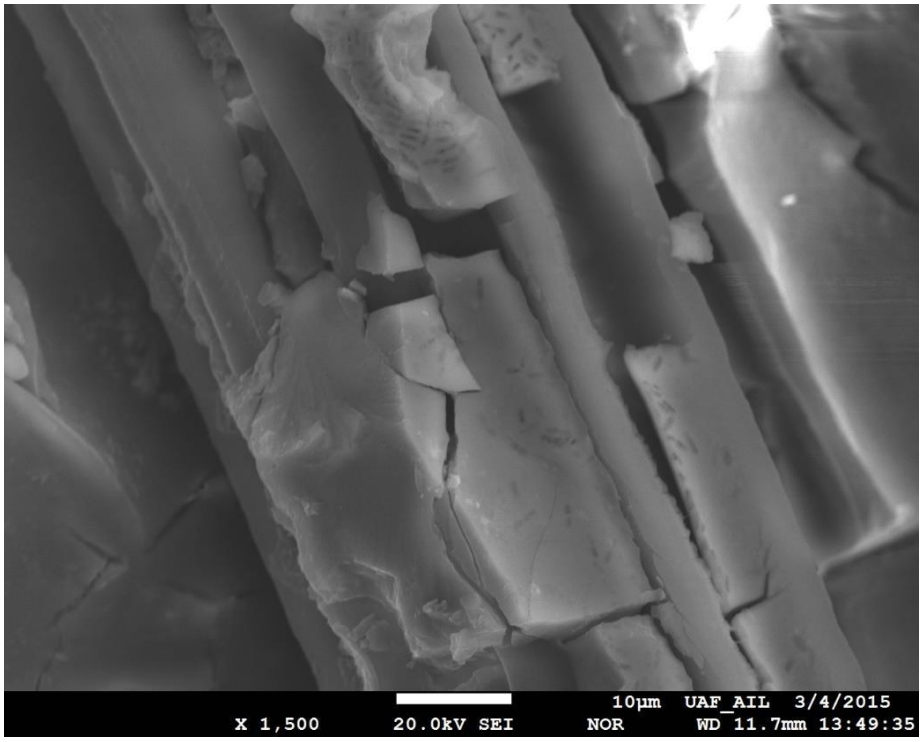

Figure 5.1 1500x photo-micrograph of wicking fiber bundle blinded by organic silt

remained completely dry throughout the test. The photo-micrographs of the wicking bundles showed the fibers were coated with the organic clay contained in the silt.

As expected, the H2Ri performed well in the flume containing the sand during all three test phases. In each case, the data indicated the fabric was capable of removing any water that was able to migrate to it. Unfortunately, the soil suction gages failed to work properly.

Perhaps the most telling indicator of the effectiveness of the wicking fabric was shown in the wetting test for the sand (case 2) where the H2Ri moved free water into the sand up to the splice. The data from all of the tests in the sand flume indicated the splices in the fabric were inefficient. This was confirmed by when the flume was disassembled. The material beneath the splice was fully saturated and free water was sitting on top of the fabric.

Based on the tests, H2Ri can be expected to work well in free draining material. However, H2Ri should not be used in organic silts. These two materials represent the extremes. Unfortunately,

no firm conclusions about clays or materials containing clay can be conclusively drawn for this data since organic clays have properties which are not necessarily indicative of other clays. However, it is likely that H2Ri will not be effective in impermeable soils since water cannot readily get to the fabric.

Splices are a concern due to the inefficiencies observed. There are two basic alternatives to resolve these issues. First, consider weaving the wicking fibers in the longitudinal direction of the fabric rather than the transverse direction. This would eliminate the need for a splice.

The second option is to develop an effective splice. The 3 foot simple overlap used in this experiment was not effective. It is doubtful that a sewn joint would be better.